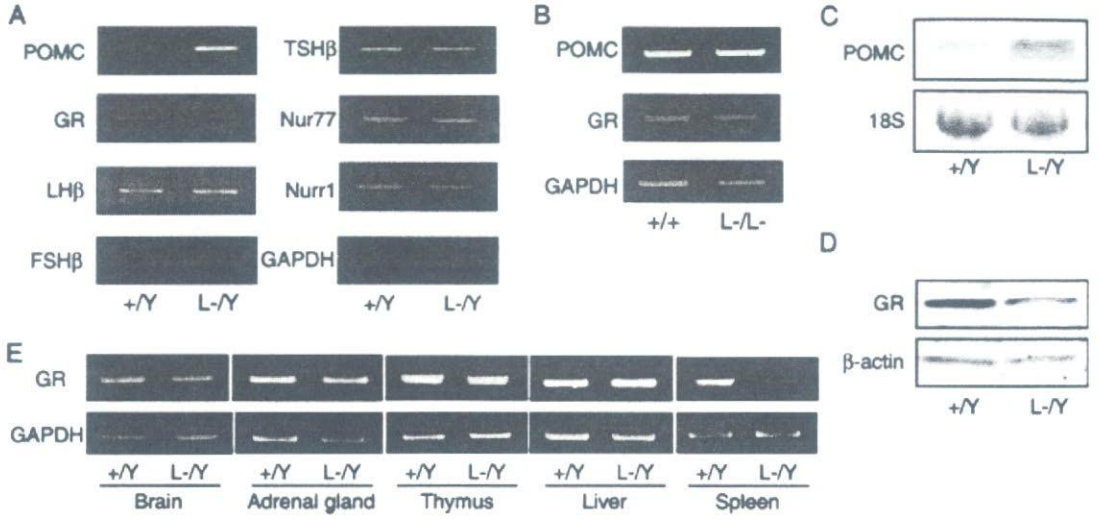

FIG. 5. Altered expression levels of gene transcripts involved in the HPA axis. (A) Increased POMC and decreased GR expression levels of transcripts in ARKO pituitary by semiquantitative RT-PCR. LHβ, luteinizing hormone β; FSHβ, follicle-stimulating hormone β; TSHβ, thyroid-stimulating hormone β. (B) No significant alterations of POMC and GR mRNA levels in the pituitary glands of female ARKO ($AR^{L-/L-}$) mice. (C and D) Northern blot analyses showing clear up-regulation of POMC mRNA levels and down-regulation of GR mRNA levels in the ARKO pituitary. (E) Tissue-specific reduction of GR transcripts in ARKO mice. GR expression levels are down-regulated only in the spleen and pituitary in male ARKO mice.

The hypertrophic and hyperplastic adrenal glands in the ARKO mice probably resulted from high levels of serum ACTH, derived from high POMC transcript levels in the pituitaries of ARKO mice. Studies with transgenic mice expressing antisense RNA against the GR in the brain and anterior pituitary demonstrate that the GR mediates the negative feedback regulation of glucocorticoid production through HPA axis activity (26, 36). Consistent with this observation, the male ARKO mice had low pituitary GR mRNA levels but no difference in the distribution of pituitary hormone-producing cells compared to WT animals. Thus, our findings suggest that the activated AR in the pituitary gland is needed to express pituitary GR at a sufficiently high level to participate in the negative feedback regulation of glucocorticoid production. The X-zone, which is considered a fetal zone, regresses during sexual maturation and reappears after gonadectomy (11). The molecular basis underlying X-zone regression during sexual maturation remains to be investigated. However, our results raise the possibility that the activated AR in adrenal glands induces X-zone repression by the induction of apoptosis. Consequently, the identification of AR target genes expressed in the X-zone is another interesting direction to pursue.

Liganded AR augments GR gene expression in the pituitary gland. We found that GR gene expression was impaired in the pituitary glands of ARKO males. We presumed that the reduced GR levels led to increased expression of the POMC gene, with subsequent high levels of serum ACTH. This idea was supported by the observation that the suppression of ACTH production by exogenous glucocorticoids was partially impaired in the ARKO mice. Moreover, the DHT-activated AR enhanced the GR mRNA levels in a pituitary cell line but not in 3T3-L1 preadipocytes. The effect of DHT was most likely mediated by a response element in an upstream region of the GR promoter exon 1B (33). Thus, the activated AR directly induces the pituitary GR in a cell-specific manner. How this is accomplished on a molecular level remains to be elucidated.

Do androgen/AR signaling disorders link with an ACTH-dependent hypercorticoid state? A hypercorticoid state in humans is well known to cause Cushing's syndrome, in which patients suffer from a number of disorders such as centripetal obesity, facial rounding, glucose intolerance, hyperinsulinemia, and impaired lipid and bone metabolism (23). Most of these lesions are a reflection of glucocorticoid-driven gluconeogenesis. The hypercorticoid state may result from either endogenous disorders or chronic treatment with exogenous glucocorticoid. Endogenous causes of Cushing's syndrome are further classified as ACTH dependent or independent (18). The ACTH-dependent syndrome is characterized by up-regulated levels of ACTH; however, the molecular basis underlying the ACTH overproduction remains to be investigated. It is possible that sex steroids are involved, but this has not yet been fully addressed.

The male ARKO mice exhibited abnormalities similar to those seen for ACTH-dependent Cushing's syndrome patients. Since we detected up-regulation of the pituitary POMC transcript, other POMC-derived peptides might have contributed to the onset of obesity in male ARKO mice. For example, α-MSH in the neurons of the hypothalamus plays a central role in appetite control and energy homeostasis (3, 4). Although we detected no clear alteration in α-MSH immunoreactivity in the arcuate nuclei of the hypothalami of male ARKO mice, it will be of interest in future experiments to examine the melanocortin receptor system in ARKO brain. In contrast to the male ARKO mice, ARKO females did not display some of the abnormalities, such as obesity. It is possible that the lack of obesity in female ARKO mice may result from activation of estrogen receptors (ERs). ERs activated by high physiological

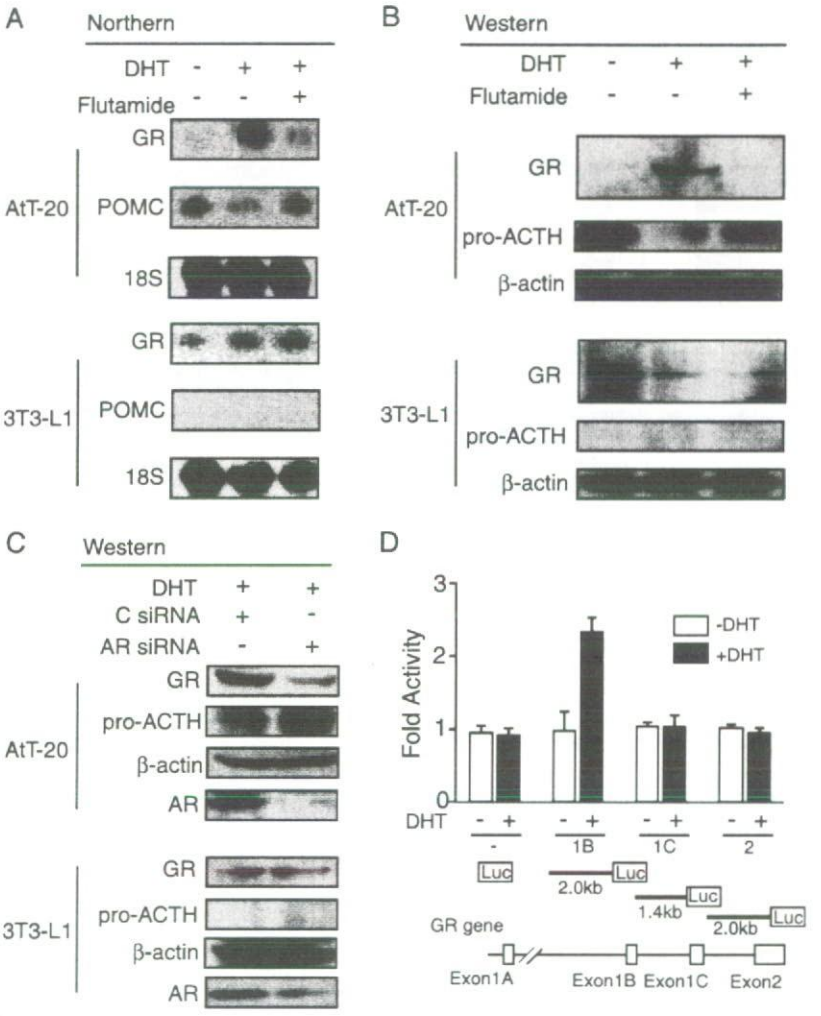

FIG. 6. Cell-type-specific regulation of the GR by activated AR. (A) Regulation of GR and POMC gene expression by treatment with either DHT or an AR antagonist (Flutamide) in the cultured cells as analyzed by Northern blot analysis. (B) Expression of the GR and pro-ACTH proteins was analyzed by Western blot analysis. (C) The significance of AR in the GR gene regulation was tested by AR RNA interference (with small interfering RNA [siRNA]) in the cultured cells. C siRNA, control siRNA. (D) Luciferase assay was performed with a series of the GR promoter regions in AtT-20 cells. After transfection with each of the promoter tk-luciferase vectors, the transfected cells were incubated with or without 10^{-7} M DHT.

levels of endogenous estrogens are effective in maintaining the proper levels of pituitary GR mRNAs needed to control POMC gene expression. This idea is indeed supported by the finding of unaltered levels of GR and POMC transcripts in the pituitary glands of the female ARKO mice. Moreover, estrogen treatment in female rats is shown to suppress serum levels of ACTH (27, 41). The common but gender-specific putative functions of the AR and ER in the brain have already been described in the context of mouse sexual behavior (24, 29). Though the possible ER functions remain to be studied for female ERKO mice, the present study suggests that the activated AR potentiates the negative HPA feedback regulation of glucocorticoid production through up-regulation of GR expression levels. Our study implies that the AR may be a potential therapeutic target for ACTH-dependent Cushing's syndrome.

In conclusion, the present study suggests that the androgen/AR signaling system is a negative pathway for glucocorticoid secretion in adult male mice. ARKO mice showed decreased GR expression in the pituitary glands and increased circulating ACTH and glucocorticoid. Androgens may increase the sensitivity of the HPA negative feedback loop to glucocorticoids by increasing GR expression in the pituitary gland, leading to suppression of adrenal cortical function. Thus, we presume that activated AR in the pituitary gland is a component of the negative feedback system for glucocorticoid production.

ACKNOWLEDGMENTS

We thank members of the KO project team for experimental support, A. F. Parlow (NIDDK, National Hormone and Peptide Program, Torrance, CA) for kindly providing antisera, and H. Higuchi for manuscript preparation.

This work was supported in part by the Program for Promotion of Basic Research Activities for Innovative Biosciences (PROBRAIN) and priority areas from the Ministry of Education, Culture, Sports, Science and Technology (to S.K.).

REFERENCES

1. **Bannister, A. J., and T. Kouzarides.** 2005. Reversing histone methylation. Nature **436:**1103–1106.
2. **Barden, N., I. S. Stec, A. Montkowski, F. Holsboer, and J. M. Reul.** 1997. Endocrine profile and neuroendocrine challenge tests in transgenic mice expressing antisense RNA against the glucocorticoid receptor. Neuroendocrinology **66:**212–220.
3. **Coll, A. P., I. S. Farooqi, B. G. Challis, G. S. Yeo, and S. O'Rahilly.** 2004. Proopiomelanocortin and energy balance: insights from human and murine genetics. J. Clin. Endocrinol. Metab. **89:**2557–2562.
4. **Cone, R. D.** 2005. Anatomy and regulation of the central melanocortin system. Nat. Neurosci. **8:**571–578.
5. **Couse, J. F., and K. S. Korach.** 1999. Estrogen receptor null mice: what have we learned and where will they lead us? Endocr. Rev. **20:**358–417.
6. **Fan, W., T. Yanase, M. Nomura, T. Okabe, K. Goto, T. Sato, H. Kawano, S. Kato, and H. Nawata.** 2005. Androgen receptor null male mice develop late-onset obesity caused by decreased energy expenditure and lipolytic activity but show normal insulin sensitivity with high adiponectin secretion. Diabetes **54:**1000–1008.
7. **Fischle, W., Y. Wang, and C. D. Allis.** 2003. Histone and chromatin cross-talk. Curr. Opin. Cell Biol. **15:**172–183.
8. **Fujiki, R., M. S. Kim, Y. Sasaki, K. Yoshimura, H. Kitagawa, and S. Kato.** 2005. Ligand-induced transrepression by VDR through association of WSTF with acetylated histones. EMBO J. **24:**3881–3894.
9. **Glass, C. K., and M. G. Rosenfeld.** 2000. The coregulator exchange in transcriptional functions of nuclear receptors. Genes Dev. **14:**121–141.
10. **Heinzel, T., R. M. Lavinsky, T. M. Mullen, M. Soderstrom, C. D. Laherty, J. Torchia, W. M. Yang, G. Brard, S. D. Ngo, J. R. Davie, E. Seto, R. N. Eisenman, D. W. Rose, C. K. Glass, and M. G. Rosenfeld.** 1997. A complex containing N-CoR, mSin3 and histone deacetylase mediates transcriptional repression. Nature **387:**43–48.
11. **Howard, J. M., J. M. Olney, J. P. Frawley, R. E. Peterson, and S. Guerra.** 1955. Adrenal function in the combat casualty. AMA Arch. Surg. **71:**47–58.
12. **Ito, T., M. Bulger, M. J. Pazin, R. Kobayashi, and J. T. Kadonaga.** 1997. ACF, an ISWI-containing and ATP-utilizing chromatin assembly and remodeling factor. Cell **90:**145–155.
13. **Kamei, Y., L. Xu, T. Heinzel, J. Torchia, R. Kurokawa, B. Gloss, S. C. Lin, R. A. Heyman, D. W. Rose, C. K. Glass, and M. G. Rosenfeld.** 1996. A CBP integrator complex mediates transcriptional activation and AP-1 inhibition by nuclear receptors. Cell **85:**403–414.
14. **Kato, S.** 2002. Androgen receptor structure and function from knock-out mouse. Clin. Pediatr. Endocrinol. **11:**1–7.
15. **Kato, S., H. Endoh, Y. Masuhiro, T. Kitamoto, S. Uchiyama, H. Sasaki, S. Masushige, Y. Gotoh, E. Nishida, H. Kawashima, et al.** 1995. Activation of the estrogen receptor through phosphorylation by mitogen-activated protein kinase. Science **270:**1491–1494.
16. **Kawano, H., T. Sato, T. Yamada, T. Matsumoto, K. Sekine, T. Watanabe, T. Nakamura, T. Fukuda, K. Yoshimura, T. Yoshizawa, K. Aihara, Y. Yamamoto, Y. Nakamichi, D. Metzger, P. Chambon, K. Nakamura, H. Kawaguchi, and S. Kato.** 2003. Suppressive function of androgen receptor in bone resorption. Proc. Natl. Acad. Sci. USA **100:**9416–9421.
17. **Kitagawa, H., R. Fujiki, K. Yoshimura, Y. Mezaki, Y. Uematsu, D. Matsui, S. Ogawa, K. Unno, M. Okubo, A. Tokita, T. Nakagawa, T. Ito, Y. Ishimi, H. Nagasawa, T. Matsumoto, J. Yanagisawa, and S. Kato.** 2003. The chromatin-remodeling complex WINAC targets a nuclear receptor to promoters and is impaired in Williams syndrome. Cell **113:**905–917.
18. **Lacroix, A., N. Ndiaye, J. Tremblay, and P. Hamet.** 2001. Ectopic and abnormal hormone receptors in adrenal Cushing's syndrome. Endocr. Rev. **22:**75–110.
19. **Li, M., A. K. Indra, X. Warot, J. Brocard, N. Messaddeq, S. Kato, D. Metzger, and P. Chambon.** 2000. Skin abnormalities generated by temporally controlled RXRalpha mutations in mouse epidermis. Nature **407:**633–636.
20. **Mangelsdorf, D. J., C. Thummel, M. Beato, P. Herrlich, G. Schutz, K. Umesono, B. Blumberg, P. Kastner, M. Mark, P. Chambon, et al.** 1995. The nuclear receptor superfamily: the second decade. Cell **83:**835–839.
21. **Murayama, A., M. S. Kim, J. Yanagisawa, K. Takeyama, and S. Kato.** 2004. Transrepression by a liganded nuclear receptor via a bHLH activator through co-regulator switching. EMBO J. **23:**1598–1608.
22. **Narlikar, G. J., H. Y. Fan, and R. E. Kingston.** 2002. Cooperation between complexes that regulate chromatin structure and transcription. Cell **108:**475–487.
23. **Newell-Price, J., X. Bertagna, A. B. Grossman, and L. K. Nieman.** 2006. Cushing's syndrome. Lancet **367:**1605–1617.
24. **Ogawa, S., A. E. Chester, S. C. Hewitt, V. R. Walker, J. A. Gustafsson, O. Smithies, K. S. Korach, and D. W. Pfaff.** 2000. Abolition of male sexual behaviors in mice lacking estrogen receptors alpha and beta (alpha beta ERKO). Proc. Natl. Acad. Sci. USA **97:**14737–14741.
25. **Ohtake, F., K. Takeyama, T. Matsumoto, H. Kitagawa, Y. Yamamoto, K. Nohara, C. Tohyama, A. Krust, J. Mimura, P. Chambon, J. Yanagisawa, Y. Fujii-Kuriyama, and S. Kato.** 2003. Modulation of oestrogen receptor signalling by association with the activated dioxin receptor. Nature **423:**545–550.
26. **Pepin, M. C., F. Pothier, and N. Barden.** 1992. Impaired type II glucocorticoid-receptor function in mice bearing antisense RNA transgene. Nature **355:**725–728.
27. **Redei, E., L. Li, I. Halasz, R. F. McGivern, and F. Aird.** 1994. Fast glucocorticoid feedback inhibition of ACTH secretion in the ovariectomized rat: effect of chronic estrogen and progesterone. Neuroendocrinology **60:**113–123.
28. **Rosenfeld, M. G., V. V. Lunyak, and C. K. Glass.** 2006. Sensors and signals: a coactivator/corepressor/epigenetic code for integrating signal-dependent programs of transcriptional response. Genes Dev. **20:**1405–1428.
29. **Sato, T., T. Matsumoto, H. Kawano, T. Watanabe, Y. Uematsu, K. Sekine, T. Fukuda, K. Aihara, A. Krust, T. Yamada, Y. Nakamichi, Y. Yamamoto, T. Nakamura, K. Yoshimura, T. Yoshizawa, D. Metzger, P. Chambon, and S. Kato.** 2004. Brain masculinization requires androgen receptor function. Proc. Natl. Acad. Sci. USA **101:**1673–1678.
30. **Sato, T., T. Matsumoto, T. Yamada, T. Watanabe, H. Kawano, and S. Kato.** 2003. Late onset of obesity in male androgen receptor-deficient (AR KO) mice. Biochem. Biophys. Res. Commun. **300:**167–171.
31. **Sekine, K., H. Ohuchi, M. Fujiwara, M. Yamasaki, T. Yoshizawa, T. Sato, N. Yagishita, D. Matsui, Y. Koga, N. Itoh, and S. Kato.** 1999. Fgf10 is essential for limb and lung formation. Nat. Genet. **21:**138–141.
32. **Shiina, H., T. Matsumoto, T. Sato, K. Igarashi, J. Miyamoto, S. Takemasa, M. Sakari, I. Takada, T. Nakamura, D. Metzger, P. Chambon, J. Kanno, H. Yoshikawa, and S. Kato.** 2006. Premature ovarian failure in androgen receptor-deficient mice. Proc. Natl. Acad. Sci. USA **103:**224–229.
33. **Strahle, U., A. Schmidt, G. Kelsey, A. F. Stewart, T. J. Cole, W. Schmid, and G. Schutz.** 1992. At least three promoters direct expression of the mouse glucocorticoid receptor gene. Proc. Natl. Acad. Sci. USA **89:**6731–6735.
34. **Suzawa, M., I. Takada, J. Yanagisawa, F. Ohtake, S. Ogawa, T. Yamauchi, T. Kadowaki, Y. Takeuchi, H. Shibuya, Y. Gotoh, K. Matsumoto, and S. Kato.** 2003. Cytokines suppress adipogenesis and PPAR-gamma function through the TAK1/TAB1/NIK cascade. Nat. Cell Biol. **5:**224–230.
35. **Takeyama, K., S. Kitanaka, T. Sato, M. Kobori, J. Yanagisawa, and S. Kato.** 1997. 25-Hydroxyvitamin D3 1alpha-hydroxylase and vitamin D synthesis. Science **277:**1827–1830.
36. **Thomas, M., M. Keramidas, E. Monchaux, and J. J. Feige.** 2004. Dual hormonal regulation of endocrine tissue mass and vasculature by adrenocorticotropin in the adrenal cortex. Endocrinology **145:**4320–4329.
37. **Wilson, J. D.** 1999. The role of androgens in male gender role behavior. Endocr. Rev. **20:**726–737.
38. **Yanagisawa, J., H. Kitagawa, M. Yanagida, O. Wada, S. Ogawa, M. Nakagomi, H. Oishi, Y. Yamamoto, H. Nagasawa, S. B. McMahon, M. D. Cole, L. Tora, N. Takahashi, and S. Kato.** 2002. Nuclear receptor function requires a TFTC-type histone acetyl transferase complex. Mol. Cell **9:**553–562.
39. **Yanagisawa, J., Y. Yanagi, Y. Masuhiro, M. Suzawa, M. Watanabe, K. Kashiwagi, T. Toriyabe, M. Kawabata, K. Miyazono, and S. Kato.** 1999. Convergence of transforming growth factor-beta and vitamin D signaling pathways on SMAD transcriptional coactivators. Science **283:**1317–1321.
40. **Yoshizawa, T., Y. Handa, Y. Uematsu, S. Takeda, K. Sekine, Y. Yoshihara, T. Kawakami, K. Arioka, H. Sato, Y. Uchiyama, S. Masushige, A. Fukamizu, T. Matsumoto, and S. Kato.** 1997. Mice lacking the vitamin D receptor exhibit impaired bone formation, uterine hypoplasia and growth retardation after weaning. Nat. Genet. **16:**391–396.
41. **Young, E. A., M. Altemus, V. Parkison, and S. Shastry.** 2001. Effects of estrogen antagonists and agonists on the ACTH response to restraint stress in female rats. Neuropsychopharmacology **25:**881–891.

Cell

Estrogen Prevents Bone Loss via Estrogen Receptor α and Induction of Fas Ligand in Osteoclasts

Takashi Nakamura,[1,2,9] Yuuki Imai,[1,3,9] Takahiro Matsumoto,[1,2] Shingo Sato,[4] Kazusane Takeuchi,[1] Katsuhide Igarashi,[5] Yoshifumi Harada,[6] Yoshiaki Azuma,[6] Andree Krust,[7] Yoko Yamamoto,[1] Hiroshi Nishina,[4] Shu Takeda,[4] Hiroshi Takayanagi,[4] Daniel Metzger,[7] Jun Kanno,[5] Kunio Takaoka,[3] T. John Martin,[8] Pierre Chambon,[7] and Shigeaki Kato[1,2,*]

[1]Institute of Molecular and Cellular Biosciences, University of Tokyo, Yayoi 1-1-1, Bunkyo-ku, Tokyo 113-0032, Japan

[2]Exploratory Research for Advanced Technology, Japan Science and Technology Agency, Honcho 4-1-8, Kawaguchi, Saitama 332-0012, Japan

[3]Department of Orthopaedic Surgery, Osaka City University Graduate School of Medicine, Asahimachi 1-4-3, Abeno-ku, Osaka, 545-8585, Japan

[4]Tokyo Medical and Dental University, Yushima 1-5-45, Bunkyo-ku, Tokyo 113-8510, Japan

[5]Division of Cellular and Molecular Toxicology, National Institute of Health Sciences, 1-18-1 Kamiyoga, Setagaya-ku, Tokyo 158-8501, Japan

[6]Teijin Institute for Biomedical Research, Asahigaoka 4-3-2, Hino, Tokyo 191-8512, Japan

[7]Institut de Génétique et de Biologie Moleculaire et Cellulaire, Departement of Physiological Genetics / Inserm, U-596 / CNRS, UMR7104 / Université Louis Pasteur, Illkirch, Strasbourg, F-67400 France

[8]St. Vincent's Institute of Medical Research, 9 Princes Street, Fitzroy VIC 3065, Australia

[9]These authors contributed equally to this work.

*Correspondence: uskato@mail.ecc.u-tokyo.ac.jp

DOI 10.1016/j.cell.2007.07.025

SUMMARY

Estrogen prevents osteoporotic bone loss by attenuating bone resorption; however, the molecular basis for this is unknown. Here, we report a critical role for the osteoclastic estrogen receptor α (ERα) in mediating estrogen-dependent bone maintenance in female mice. We selectively ablated ERα in differentiated osteoclasts ($ER\alpha^{\Delta Oc/\Delta Oc}$) and found that $ER\alpha^{\Delta Oc/\Delta Oc}$ females, but not males, exhibited trabecular bone loss, similar to the osteoporotic bone phenotype in postmenopausal women. Further, we show that estrogen induced apoptosis and upregulation of Fas ligand (FasL) expression in osteoclasts of the trabecular bones of WT but not $ER\alpha^{\Delta Oc/\Delta Oc}$ mice. The expression of ERα was also required for the induction of apoptosis by tamoxifen and estrogen in cultured osteoclasts. Our results support a model in which estrogen regulates the life span of mature osteoclasts via the induction of the Fas/FasL system, thereby providing an explanation for the osteoprotective function of estrogen as well as SERMs.

INTRODUCTION

Bone remodeling is a dynamic metabolic process. The destruction or "resorption" of pre-existing bone by mature osteoclasts is followed by the formation of new bone by osteoblasts. Osteoblasts are derived from pleiotropic mesenchymal stem cells in the bone marrow. Mature osteoclasts are multinuclear, macrophage-like cells, derived from hematopoietic stem cells also in the bone marrow. Bone resorption and deposition are tightly coupled, and their balance defines both bone mass as well as quality. The regulation of bone remodeling is complex. A number of systemic hormones and transcription factors directly regulate the proliferation and differentiation of osteoblasts and osteoclasts (Karsenty, 2006; Karsenty and Wagner, 2002; Rodan and Martin, 2000; Teitelbaum and Ross, 2003). Additionally, the indirect cellular communication among groups of bone cells is also physiologically critical for bone growth and remodeling (Martin and Sims, 2005; Mundy and Elefteriou, 2006). The molecular and genetic mechanisms governing bone cell fate have been intensively studied; however, how the life span of bone cells is determined on a molecular level remains elusive.

Estrogen is a key hormone in bone remodeling in several species. The osteoprotective action of estrogen is demonstrable in rodents and is clinically important in humans, particularly older women (Chien and Karsenty, 2005;

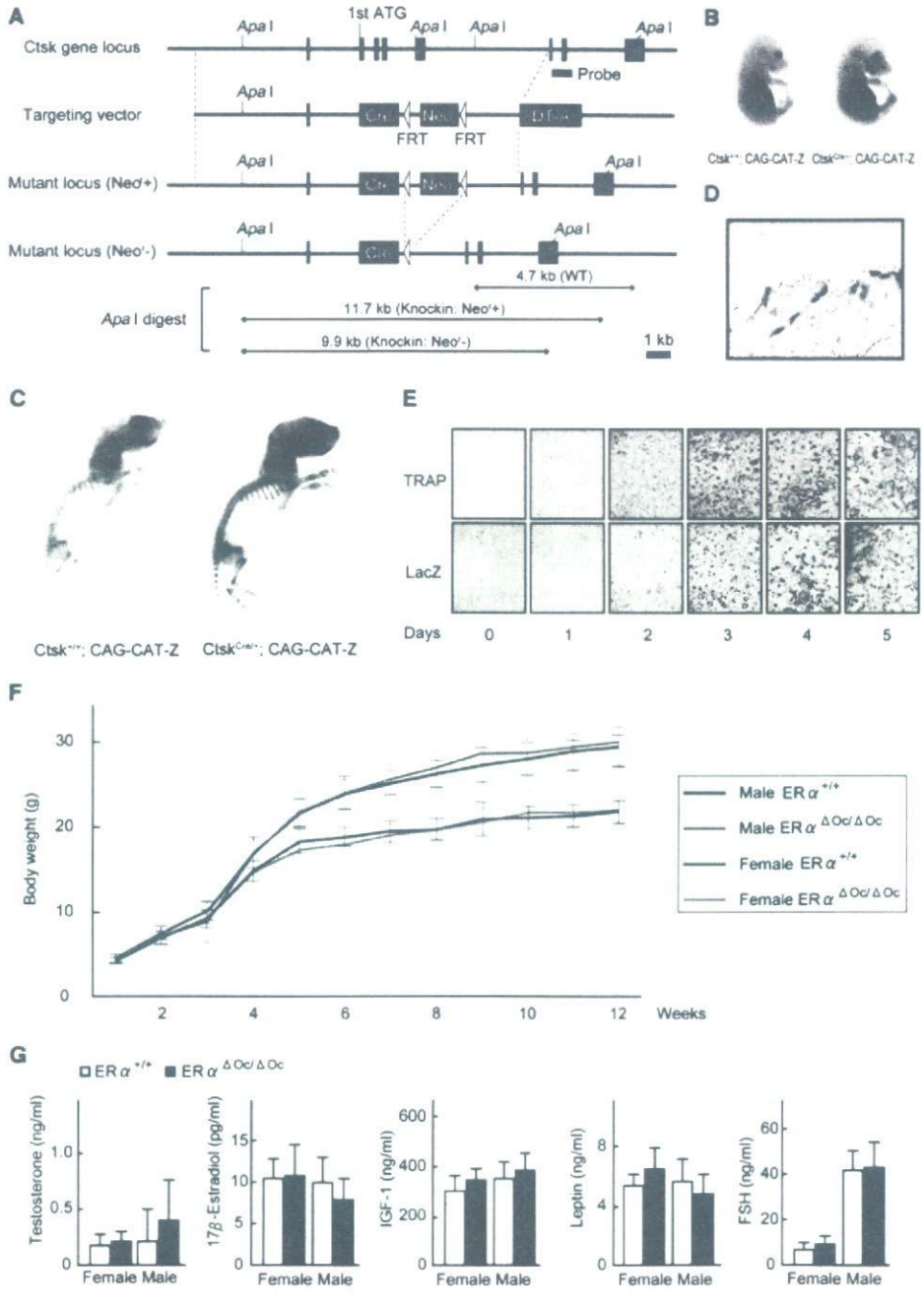

Figure 1. Generation of Knockin Mice Selectively Expressing Cre in Mature Osteoclasts

(A) Illustration of the targeting strategy for insertion of the *Cre* gene into the mouse *Cathepsin K* (*Ctsk*) gene. A targeting vector was generated to contain the *Cre* cDNA at the endogenous ATG start site, followed by a *FRT* (Flp-recombinase target)-flanked *Neo*^{r} cassette. The *DT-A* (diphtheria toxin-A) gene was also inserted to avoid random integrations.

(B and C) *Ctsk-Cre* mice were then crossed with *CAG-CAT-Z* mice. β-galactosidase activity derived from the activated *LacZ* reporter gene was monitored to test if expressed Cre excised the *lox*P sites in mature osteoclasts. LacZ expression patterns reflected the localization patterns of mature osteoclasts in the developing bone at 16.5 days post coitum embryos and in the skeletal tissues of 7-day-old pups.

(D) The LacZ expression induced by Cre-mediated excision was also seen in osteoclasts attached to trabecular bone in the lumber vertebrae of 12-week-old mice.

(E) LacZ expression was induced during osteoclastogenesis. Osteoclast-like cells that differentiated from bone-marrow macrophages following culture in the presence of M-CSF and RANKL were stained with TRAP (tartrate-resistant acid phosphatase), a mature osteoclast marker.

Delmas, 2002; Raisz, 2005; Rodan and Martin, 2000). Estrogen deficiency in postmenopausal women frequently leads to osteoporosis, the most common skeletal disorder. Similarly, ovariectomy clearly produces an osteoporotic bone phenotype in mice. Osteoporotic bone loss is the result of high bone turnover in which bone resorption outpaces bone deposition (Rodan and Martin, 2000; Teitelbaum, 2007). This imbalance in bone turnover that is induced by estrogen deficiency in women and female rodents can be ameliorated with bio-available estrogens including selective estrogen receptor modulators (SERMs) (Riggs and Hartmann, 2003).

Estrogen and SERMs primarily act by regulating gene transcription via estrogen receptors (ERα, ERβ) (Couse and Korach, 1999; Shang and Brown, 2002). ERs belong to the nuclear receptor gene superfamily and act as ligand-inducible transcriptional factors (Mangelsdorf et al., 1995). ER dimers directly or indirectly associate with specific DNA elements in the target gene promoter (Shang and Brown, 2002) and control transcription through reorganizing chromatin structure and histone modifications (Belandia and Parker, 2003). Genetic mouse models (KO mice) lacking ERα ($ER\alpha^{-/-}$) and ERβ ($ER\beta^{-/-}$) provide insights into ER function (Mueller and Korach, 2001; Windahl et al., 2002). In mice, though ERα appears to be the major receptor in most estrogen target tissues including bone (Sims et al., 2003), neither clear bone loss nor high bone turnover is detectable in ERα single or ERα/ERβ double-KO females (Syed and Khosla, 2005; Windahl et al., 2002). This unexpected maintenance of bone mass in female mutants is presumed to be due to unphysiologically elevated levels of other osteoprotective hormones, like androgens. Systemic defects in the hypothalamus caused by ER inactivation appear to impair the negative feedback system of hormone production (Syed and Khosla, 2005). This leads to an excess in estrogen precursors, notably androgens. In fact, the anabolic effects of androgens mediated by the androgen receptor (AR) are evident in female mice (Kawano et al., 2003; Sims et al., 2003). In males, estrogen is also osteoprotective, as is evident by the development of osteopenia in male patients genetically deficient in ERα (Smith et al., 1994) or aromatase activity (Simpson and Davis, 2001). Thus, irrespective of the accumulating clinical and basic research data on the osteoprotective actions of estrogen and SERMs, the molecular basis of this osteoprotection in females remains elusive.

To study the molecular interactions behind the antibone resorptive actions of estrogen in women and female animals, we genetically ablated ERα in mature osteoclasts ($ER\alpha^{\Delta Oc/\Delta Oc}$). Selective ablation of ERα in differentiated osteoclasts ($ER\alpha^{\Delta Oc/\Delta Oc}$) was accomplished by crossing a *Cathepsin K-Cre* knockin mouse with a floxed *ERα* mouse. This resulted in clear trabecular bone loss and high bone turnover associated with increased osteoclast numbers in females but not in males. In the female mutants, further bone loss following ovariectomy was not significant and recovery by estrogen was ineffective in the trabecular areas of long bones and lumbar vertebral bodies. Upregulated expression of *Fas ligand* (*FasL*) gene, and increased apoptosis in differentiated osteoclasts by estrogen was found in the intact bone of wild-type females but undetectable in $ER\alpha^{\Delta Oc/\Delta Oc}$ females. Induction of FasL and apoptosis by estrogen as well as a SERM also required ERα in cultured osteoclasts. Thus, we propose that the osteoprotective actions of estrogen and SERMs are mediated at least in part through osteoclastic ERα in trabecular bone, and the life span of mature osteoclasts is regulated through the activation of the FasL signaling.

RESULTS

Generation of Osteoclast-Specific *ERα* Gene Disruption by Knocked-In *Cre* in the *Cathepsin K* Gene

To specifically disrupt *ERα* gene in mature osteoclasts, we knocked in *Cre* into the gene locus of *Cathepsin K* ($Ctsk^{Cre/+}$) (Figures 1A, S1A, and S1B), a gene known to be expressed in differentiated osteoclastic cells arising from hematopoietic stem cells. This gene is functionally indispensable for mature osteoclasts (Saftig et al., 1998). Only one copy appears enough to support normal bone formation and bone turnover, since heterozygous mutant mice of *Cathepsin K* ($Ctsk^{+/-}$) have no obvious bone phenotype (Gowen et al., 1999; Li et al., 2006; Saftig et al., 1998) . Clear, bone-specific expression of the *Cre* transcript in the adult $Ctsk^{Cre/+}$ mice was observed in the tested tissues (Figure S1C). To confirm Cre protein expression, the $Ctsk^{Cre/+}$ mice were crossed with tester mice (*CAG-CAT-Z*). These mice were genetically engineered to express β-galactosidase by excision of the transcribed stop sequence in front of the *β-galactosidase* gene (*LacZ*) in cells expressing Cre (Sakai and Miyazaki, 1997). β-galactosidase expression visualized by LacZ staining was observed in the bones of 16.5 dpc embryos and 7-day-old pups of $Ctsk^{Cre/+}$; *CAG-CAT-Z* mice. Expression patterns were consistent with the appearance and skeletal localization of functionally mature osteoclasts (Figures 1B and 1C). Histochemical staining of LacZ in the lumbar vertebrae of 12-week-old mice was localized in multinuclear osteoclasts (Figure 1D) but not seen in osteoblasts and osteocytes (Figure S1D) and the hypothalamus (Figure S1E). Since *Cathepsin K* gene expression is evident in differentiated osteoclasts (Saftig et al., 1998), we used an in vitro culture cell system to test whether Cre expression was driven by the endogenous promoter that is induced at the time of osteoclast differentiation. Osteoclast-precursor cells derived from bone marrow

(F) The growth curve of $ER\alpha^{\Delta Oc/\Delta Oc}$ mice was indistinguishable from that of the control mice. Data are represented as mean ± SEM.
(G) Serum hormone levels were normal in 12-week-old $ER\alpha^{\Delta Oc/\Delta Oc}$ (filled column) versus $ER\alpha^{+/+}$ (open column) mice (n = 10–11 animals per genotype). Data are represented as mean ± SEM.

were cytodifferentiated for 1 week in the presence of M-CSF (macrophage colony stimulating factor) and RANKL (receptor activator of NFκB ligand) (Koga et al., 2004). TRAP-positive osteoclasts emerged after 3 days of culture (Figure 1E). The number of TRAP-positive osteoclasts and the number of LacZ-expressing cells simultaneously increased. In the contrast, the LacZ expression was not detected in primary cultured osteoblasts derived from the calvaria (Figure S1F). In view of both our in vivo and in vitro observations, we conclude that the $Ctsk^{Cre/+}$ mouse line expresses Cre in differentiated osteoclasts. Moreover, estrogen response in bone mass control was not distinguishable in between $Ctsk^{Cre/+}$ and $Ctsk^{+/+}$ mice (Figure S2A).

We then crossed floxed $ER\alpha$ mice (Dupont et al., 2000) with $Ctsk^{Cre/+}$ mice to disrupt ERα in differentiated osteoclasts ($ER\alpha^{\Delta Oc/\Delta Oc}$). Excision of the $ER\alpha$ gene (Figure S1G) was confirmed by Southern blotting of DNA from adult female and male (data not shown) bone as well as in cultured mature osteoclasts (Figure S1H). No overt differences were observed in the growth curve, reproduction, or tissues for up to 12 weeks of age (Figure 1F) between the $Ctsk^{Cre/+}$; $ER\alpha^{+/+}$ ($ER\alpha^{+/+}$) and the $Ctsk^{Cre/+}$; $ER\alpha^{flox/flox}$ ($ER\alpha^{\Delta Oc/\Delta Oc}$) mice, with the exception of the female bones. Serum levels of sex hormones and bone remodeling regulators such as IGF-I, leptin, and follicle-stimulating hormone (Sun et al., 2006; Takeda et al., 2002) appeared unchanged in both male and female $ER\alpha^{\Delta Oc/\Delta Oc}$ mice at 12 weeks (Figure 1G).

Osteopenia Occurred in Osteoclast-Specific ERα KO Females But Not Males

The 12-week-old $ER\alpha^{\Delta Oc/\Delta Oc}$ females exhibited a clear reduction in bone mineral density (BMD) in the femurs (Figures 2A–2C) and tibiae (data not shown) when compared with $ER\alpha^{+/+}$ mice. Though cortical bone appeared unaffected, trabecular bone loss (Figure 2A) with significant reduction of trabecular bone volume (BV/TV) (Figure 2F) was clearly seen. This is similar to the osteoporotic abnormalities observed in women during natural menopause or following ovariectomy (Delmas, 2002; Tolar et al., 2004). However, unlike men deficient in aromatase or ERα activity (Simpson and Davis, 2001; Smith et al., 1994), $ER\alpha^{\Delta Oc/\Delta Oc}$ males unexpectedly exhibited no clear bone loss even in the trabecular areas (Figures 2A–2C). In $ER\alpha^{\Delta Oc/\Delta Oc}$ females, both the bone-formation rate, estimated by double-calcein labeling (Figure 2D), as well as the bone-resorption rate, estimated from TRAP-positive differentiated osteoclast numbers (Figure 2E), were increased, indicating high bone turnover. Histomorphometric analyses of $ER\alpha^{\Delta Oc/\Delta Oc}$ females supported the observation of accelerated bone resorption, as increased numbers of osteoclasts (Oc. S/BS and N. Oc/BS) were observed together with more eroded bone surface (ES/BS in Figure 2F). Bone formation was also enhanced as the rates of mineral apposition (MAR) and bone formation (BFR/BS) were both upregulated without an increase in osteoblast numbers (Ob.S/BS) (Figure 2F). Thus, considering all of these findings, it is conceivable that the increased number of differentiated osteoclasts following ERα ablation accelerates bone resorption over formation, leading to bone loss in the trabecular areas.

No Further Bone Loss Results from Estrogen Deficiency in $ER\alpha^{\Delta Oc/\Delta Oc}$ Females

To verify whether osteoclastic ERα indeed mediates osteoprotective estrogen actions, estrogen action was investigated by ovariectomy (OVX) of 12-week-old female mice. As expected, OVX in $ER\alpha^{+/+}$ females resulted in significantly reduced BMD particularly in the trabecular bone (Figures 3A and 3B) but not in the cortical bone (Figure 3C). Consistent with previous reports, (Kimble et al., 1995; Teitelbaum and Ross, 2003), estrogen deficiency following OVX upregulated the serum levels of cytokines like TNFα and IL-1α (Figure 3D). These cytokines enhance bone resorption through stimulation of osteoclastogenesis, leading to the loss of bone mass (Teitelbaum and Ross, 2003). OVX did not further reduce BMD or trabecular bone volume of the femurs of $ER\alpha^{\Delta Oc/\Delta Oc}$ females (Figure 3B) nor affect increased number of TRAP-positive osteoclasts (see lower panel in Figure 3A) despite upregulation of serum cytokines. This suggests that the expression of cytokines known to regulate bone resorption is not under the control of osteoclastic ERα.

Estrogen Treatment Failed to Rescue the Osteoporotic Bone Phenotype of $ER\alpha^{\Delta Oc/\Delta Oc}$ Mice

Estrogen treatment by estrogen pellet implantation (OVX + E2) for 2 weeks after OVX in $ER\alpha^{+/+}$ mice elicited a dramatic increase in bone mass in both the trabecular and cortical areas of the femurs (data not shown) and lumbar vertebral bodies (Figure 4A). Estrogen action during E2 treatment in female mutants ($ER\alpha^{\Delta Oc/\Delta Oc}$) was not as pronounced as in the $ER\alpha^{+/+}$ females (Figures 4A and 4B), and the increase in the trabecular portions of the distal femurs was slight (data not shown). Histomorphometric analysis of the lumbar vertebral bodies (Figure 4B) supported the idea that E2 treatment in the female mutants was not sufficient to suppress accelerated bone resorption. These in vivo findings in the $ER\alpha^{\Delta Oc/\Delta Oc}$ females suggest that in at least the trabecular areas of the long bones and lumbar vertebral bodies, the osteoprotective estrogen action is primarily mediated via osteoclastic ERα inhibiting bone resorption.

To further test this hypothesis, we investigated ERα protein expression in mature osteoclasts from trabecular bone. Few reports document osteoclastic expression of ERα protein and an estrogen response in both intact animals and in in vitro cultured osteoclasts (Bland, 2000). We therefore reasoned that ER expression ceases during differentiation into mature cells from primary cultures of osteoclast precursors, similar to that observed in other primary culture cell systems such as avian oviduct cells, in which ERα protein expression is drastically decreased during culture (Kato et al., 1989). Using highly sensitive immunohistochemistry, we investigated whether

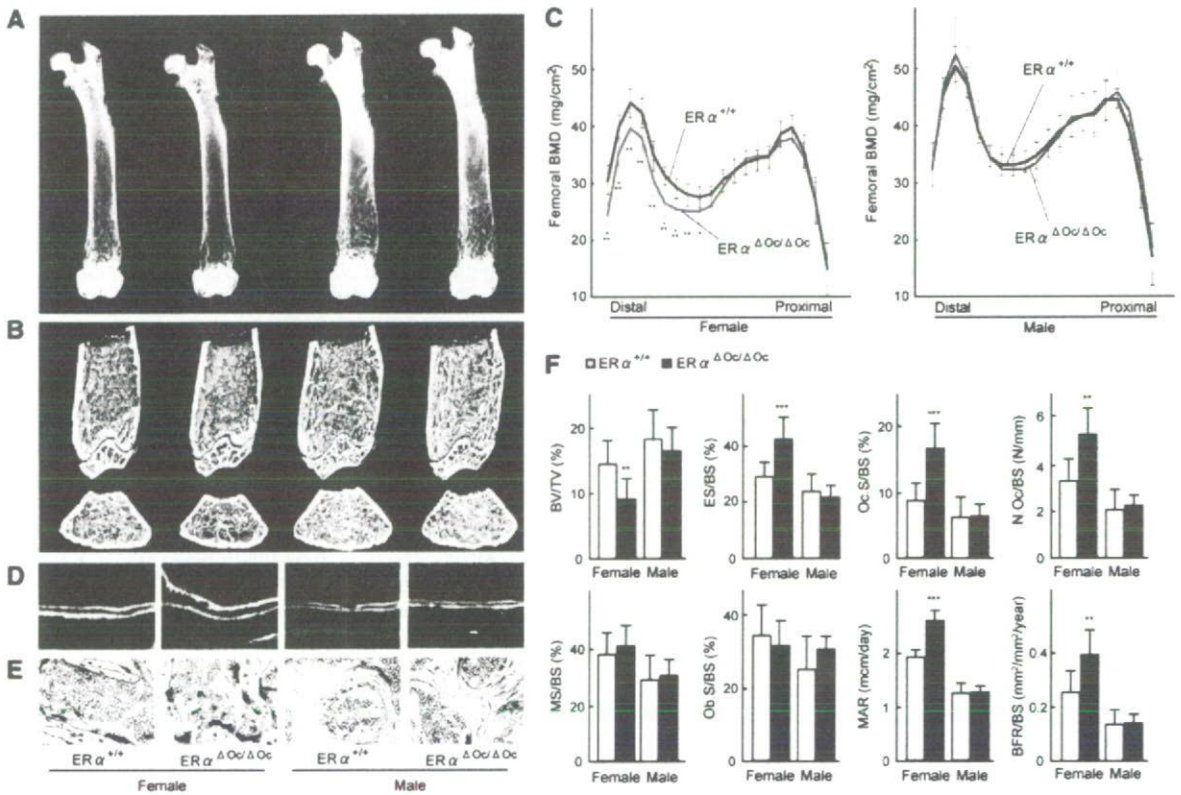

Figure 2. High Bone Turnover Osteopenia Was Observed in $ER\alpha^{\Delta Oc/\Delta Oc}$ Females But Not Males

(A) Soft X-ray images of femurs from 12-week-old $Ctsk^{Cre/+}$; $ER\alpha^{flox/flox}$ ($ER\alpha^{\Delta Oc/\Delta Oc}$) mice.

(B) Three-dimensional computed tomography images of the distal femurs and axial sections of distal metaphysis from representative 12-week-old $Ctsk^{Cre/+}$; $ER\alpha^{+/+}$ ($ER\alpha^{+/+}$) and $ER\alpha^{\Delta Oc/\Delta Oc}$ mice.

(C) BMD of each of 20 equal longitudinal divisions of femurs from 12-week-old $ER\alpha^{-/+}$ and $ER\alpha^{\Delta Oc/\Delta Oc}$ mice. (n = 10–11 animals per genotype; Student's t test, *$p < 0.05$; **$p < 0.01$; ***$p < 0.001$). Data are represented as mean ± SEM.

(D) Bone formation was also accelerated in $ER\alpha^{\Delta Oc/\Delta Oc}$ females when two calcein-labeled mineralized fronts visualized by fluorescent micrography were measured in the proximal tibia of 12-week-old mice.

(E) The number of TRAP-positive osteoclasts in the lumbar spine of female mice was increased by selective disruption of ERα in osteoclasts, indicating enhanced bone resorption.

(F) Bone turnover parameters as measured by dynamic bone histomorphometry after calcein labeling indicated high bone turnover in $ER\alpha^{\Delta Oc/\Delta Oc}$ females. Parameters are measured in the proximal tibia of 12-week-old $ER\alpha^{+/+}$ (open column) and $ER\alpha^{\Delta Oc/\Delta Oc}$ (filled column) mice. BV/TV: bone volume per tissue volume. ES/BS: eroded surface per bone surface. Oc.S/BS: osteoclast surface per bone surface. N.Oc/BS: osteoclast number per bone surface. MS/BS: mineralizing surface per bone surface. Ob.S/BS: osteoblast surface per bone surface. MAR: mineral apposition rate. BFR/BS: bone formation rate per bone surface (n = 10–11 animals per genotype; Student's t test, *$p < 0.05$; **$p < 0.01$; ***$p < 0.001$). Data are represented as mean ± SEM.

ERα protein expresses in differentiated osteoclasts in the bone tissues of femur sections from 12-week-old mice. ERα protein expression appeared abundant in osteoblasts and osteocytes of femur sections (Figure 4C) as well as hypothalamus (Figure S2B) from 12-week-old mice, in agreement with a previous report (Zaman et al., 2006). Likewise, expression levels of ERα in primary cultured osteoblasts derived from calvaria of $ER\alpha^{\Delta Oc/\Delta Oc}$ females appeared unaffected (Figure S2C). In contrast, in differentiated osteoclasts of the same femur sections, ERα expression was definitely detectable but very low in the $ER\alpha^{+/+}$ but undetectable in $ER\alpha^{\Delta Oc/\Delta Oc}$ females (Figure 4C).

Signaling by Osteoclastogenic Factors and Osteoclastogenesis Is Intact in Osteoclasts Deficient in ERα

It is possible that the osteoprotective function of osteoclastic ERα inhibits osteoclastogenesis. To address this issue, osteoclastogenesis was tested in cultured osteoclasts derived from bone-marrow cells of $ER\alpha^{\Delta Oc/\Delta Oc}$ mutants. In this cell culture system, a possible contribution of contaminated immune cells and stromal cells could be excluded, since osteoclastogenesis is only inducible by M-CSF treatment followed by M-CSF + RANKL (Koga et al., 2004).

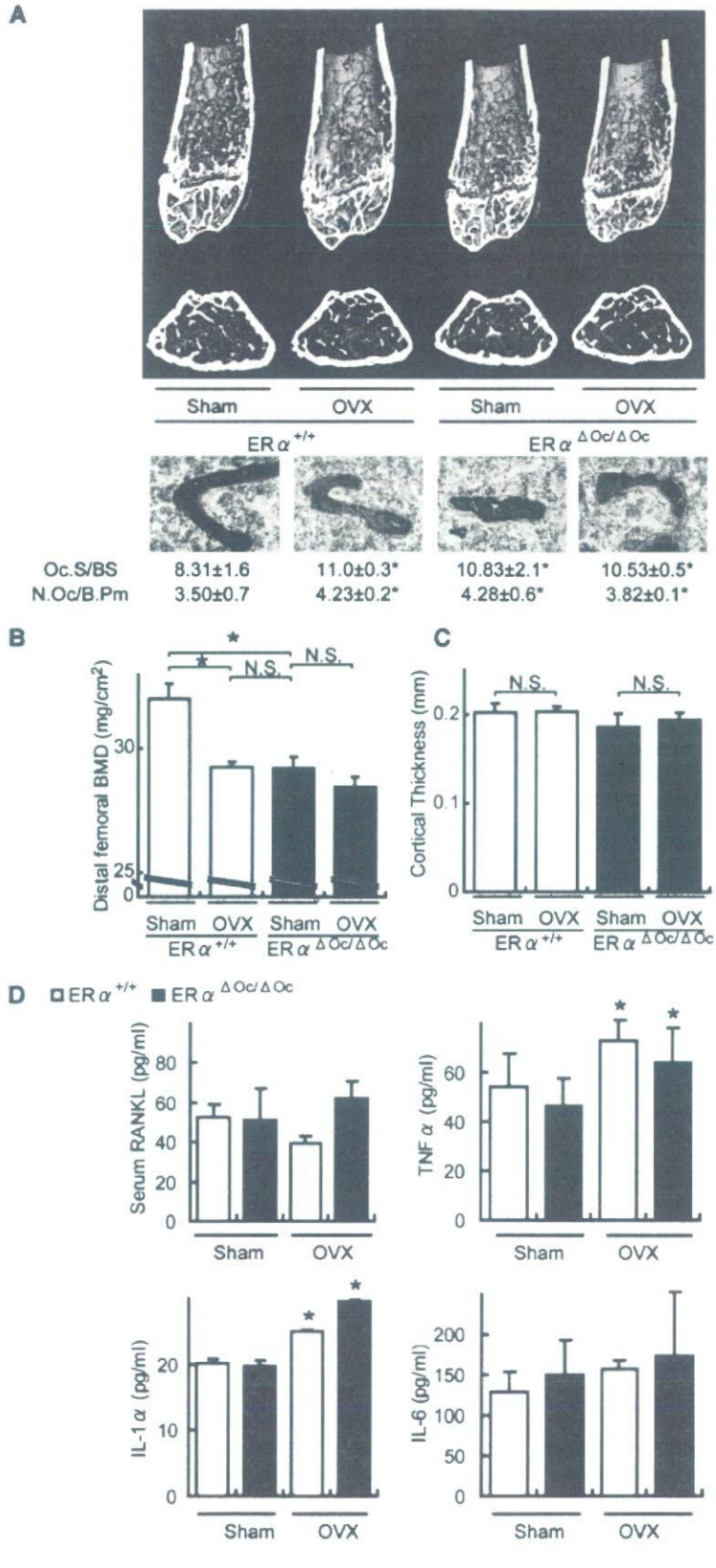

Figure 3. No Further Bone Loss of $ER\alpha^{\Delta Oc/\Delta Oc}$ Females by Ovariectomy

(A) Distal femoral micro CT analysis and lumbar vertebral bone histomorphometrical analysis of sham-operated or ovariectomized (OVX) 12-week-old $ER\alpha^{+/+}$ and $ER\alpha^{\Delta Oc/\Delta Oc}$ mice (*$p < 0.05$ compared to $ER\alpha^{+/+}$ sham group). Two weeks after OVX, the bone phenotype was analyzed.

(B) BMD of the distal femurs within each group are described in Figure 3A (*$p < 0.05$; N.S., not significant). Data are represented as mean ± SEM.

(C) Cortical thickness evaluation from micro CT analysis of femurs within each group described in Figure 3A. Data are represented as mean ± SEM.

(D) The levels of TNFα, IL-1α, and IL-6 in the bone-marrow cells culture media and serum RANKL (*$p < 0.05$ compared to each sham group). Data are represented as mean ± SEM.

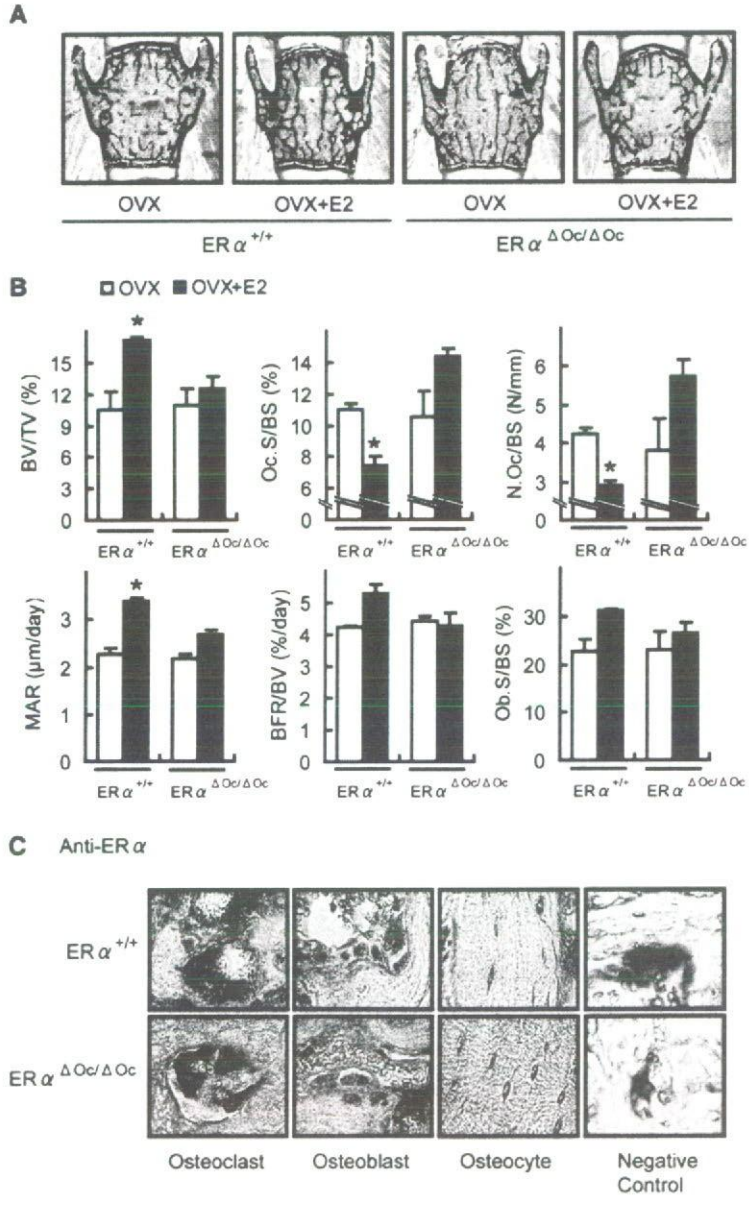

Figure 4. Estrogen treatment failed to reverse trabecular bone loss of ovariectomized $ER\alpha^{\Delta Oc/\Delta Oc}$ females

(A) von kossa staining of lumbar vertebral bodies of ovariectomized $ER\alpha^{+/+}$ and $ER\alpha^{\Delta Oc/\Delta Oc}$ mice treated with or without 17β-estradiol (0.83 μg/day) for 2 weeks (+E2) groups.

(B) Bone histomorphometrical analyses of the lumber vertebral bodies of 12-week-old ovariectomized $ER\alpha^{+/+}$ (left columns) and $ER\alpha^{\Delta Oc/\Delta Oc}$ (right columns) mice with (filled columns) or without (open columns) E2 treatment for 2 weeks (*$p < 0.05$ compared with E2-treated ovariectomized $ER\alpha^{\Delta Oc/\Delta Oc}$ mice). BV/TV: bone volume per tissue volume. ES/BS: eroded surface per bone surface. Oc.S/BS: osteoclast surface per bone surface. N.Oc/BS: osteoclast number per bone surface. MS/BS: mineralizing surface per bone surface. Ob.S/BS: osteoblast surface per bone surface. MAR: mineral apposition rate. BFR/BS: bone formation rate per bone surface. Data are represented as mean ± SEM.

(C) Immunochemical identification of ERα (brown) in TRAP-positive (red) differentiated osteoclasts. The femurs of 12 week-old mice were used for the immunodetection of ERα in bone cells. All labels were abolished when the primary antibody was preadsorbed with the immunizing peptide (negative control).

The number of TRAP-positive osteoclasts differentiated from the bone-marrow cells of $ER\alpha^{\Delta Oc/\Delta Oc}$ females was almost the same as that from $ER\alpha^{+/+}$ females (Figure 5A) and males (data not shown). The differentiated $ER\alpha^{\Delta Oc/\Delta Oc}$ osteoclasts had typical osteoclastic features, including the characteristic cell shape, TRAP-positive, multiple nuclei, and actin-ring formation, and were indistinguishable from the $ER\alpha^{+/+}$ osteoclasts (Figure 5B).

The expression levels of the prime osteoclastogenic transcription factors, c-*fos* and *NFATc1*, were unaltered by ERα deficiency in differentiated osteoclasts (Figure 5C). Furthermore, responses to RANKL in intracellular signaling, as represented by phosphorylation of p38 and IκB, were unaffected in $ER\alpha^{\Delta Oc/\Delta Oc}$ osteoclasts from females (Figure 5D) as well as males (data not shown). In light of these findings, it is unlikely that activated ERα in osteoclastic cells attenuates osteoclastogenesis.

Activation of the Fas/FasL System by Estrogen in Intact Bone Is Impaired by Osteoclastic ERα Deficiency

To examine osteoclastic ERα function in intact bone, DNA microarray analysis following real-time RT-PCR of RNA from the femurs of ovariectomized $ER\alpha^{\Delta Oc/\Delta Oc}$ females treated with or without estrogen, was performed. During

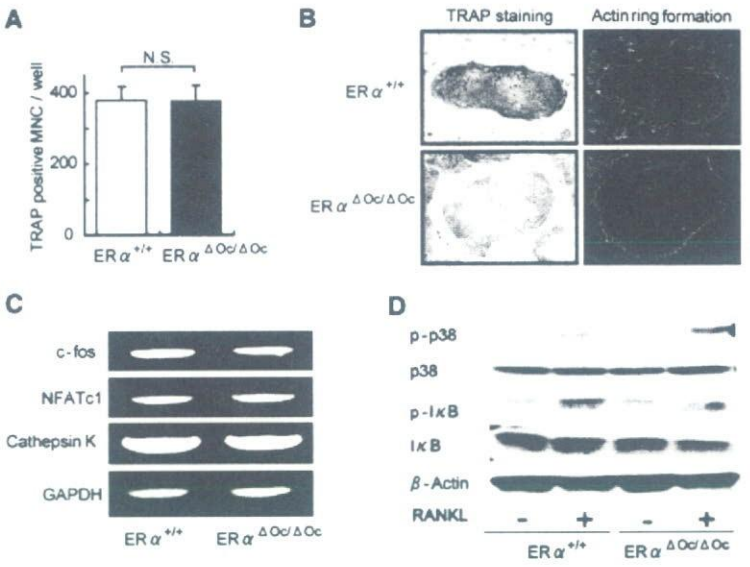

Figure 5. ERα Deficiency Did Not Affect Osteoclastogenesis

(A) TRAP-positive multinucleated cell count at 3 days after RANKL stimulation, cultured in 24-well plates (n = 6, N.S., not significant). Data are represented as mean ± SEM.

(B) TRAP staining and actin ring formation of RANKL induced primary cultured osteoclasts from bone-marrow cells of $ERα^{+/+}$ and $ERα^{ΔOc/ΔOc}$ mice.

(C) RT-PCR analysis of genes related to osteoclastogenesis.

(D) Western blot analysis of phosphorylated p38, JNK, and IκB of primary cultured bone-marrow cells stimulated with or without 100 ng/ml of RANKL for 15 min.

the search for candidate ERα target genes in bone by DNA microarray analysis (Figure S3), we found that a number of apoptosis-related factors were regulated by estrogen in the intact bone of $ERα^{+/+}$ females but dysregulated in $ERα^{ΔOc/ΔOc}$ females. This observation is consistent with a previous report of estrogen-induced apoptosis of mature osteoclasts (Kameda et al., 1997). Real-time RT-PCR to validate the estrogen regulations of the candidate genes revealed that gene expression of *FasL*, an apoptotic factor, was responsive to E2 (Figure 6A). Estrogen treatment (+E2) indeed induced expression of FasL protein in bone of ovariectomized $ERα^{+/+}$, but this induction was not obvious in ovariectomized $ERα^{ΔOc/ΔOc}$ mice (Figures 6B and 6C). Reflecting FasL induction by estrogen, estrogen-induced apoptosis (as observed by the TUNEL assay) in TRAP-positive mature trabecular osteoclasts in the distal femurs of the $ERα^{+/+}$ mice was detected, but this E2 response was abolished in the $ERα^{ΔOc/ΔOc}$ mice (Figure 6D). Furthermore, in mice lacking functional FasL ($FasL^{gld/gld}$), neither enhanced bone resorption nor bone mass loss was induced by ovariectomy (Figures 6E and 6F).

Osteoclastic ERα Mediates Estrogen-Induced apoptosis by FasL

The expression level of ERα protein in differentiated osteoclasts derived from bone marrow cells was very low, but induction of *FasL* gene expression was also detectable in the cultured osteoclasts of $ERα^{+/+}$ females as well as males (Figure 7A). However, this E2 response was impaired in cultured osteoclasts from $ERα^{ΔOc/ΔOc}$ females (Figure 7A). It is notable that such responses are also induced by tamoxifen (Figure 7C), which is an osteoprotective SERM (Harada and Rodan, 2003). ERα overexpression augmented *FasL* gene expression in response to estrogen in cultured osteoclasts from $ERα^{ΔOc/ΔOc}$ females (Figure S4A). In primary cultured calvarial osteoblasts from females as well as males (Suzawa et al., 2003), *FasL* gene induction by E2 and tamoxifen was also seen; however, it was not accompanied by increased apoptosis (data not shown). Thus, it appears that estrogen-induced apoptosis in osteoclasts is mediated by FasL expression in osteoclasts in the trabecular bone areas, presumably as well as in osteoblasts in cortical bone areas. As expected, the cell number of TUNEL-positive osteoclasts was increased by E2 in the cultured osteoclasts from $ERα^{+/+}$ females, but E2-induced apoptosis was undetectable in $ERα^{ΔOc/ΔOc}$ osteoclasts (Figure 7B). Consistent with FasL-induced apoptosis, *Fas* gene expression was observed (Figure 7D), but it was likely that Fas expression did not require ERα function (Figures S4B and S4C). Expression levels of *Fas* and *ERα* as well as E2 response in apoptosis appeared to fluctuate during osteoclast differentiation (Figures S4B–S4D); however, in FasL mutant ($FasL^{gld/gld}$) females, the E2-induced apoptosis was abolished (Figure S4E). These findings suggest that activated ERα in differentiated osteoclasts induces apoptosis through activating FasL/Fas signaling. This leads to suppression of bone resorption through truncating the already short life span of differentiated osteoclasts (Teitelbaum, 2006).

DISCUSSION

Selective ablation of ERα in mature osteoclasts in female mice shows that the osteoprotective effect of estrogen is mediated by osteoclastic ERα, at least in the trabecular regions of the tibiae, femur, and lumbar vertebrae of female mice. Activated ERα by estrogen as well as SERMs appears to truncate the already short life span (estimated at 2 weeks) of differentiated osteoclasts by inducing apoptosis through activation of the Fas/FasL system.

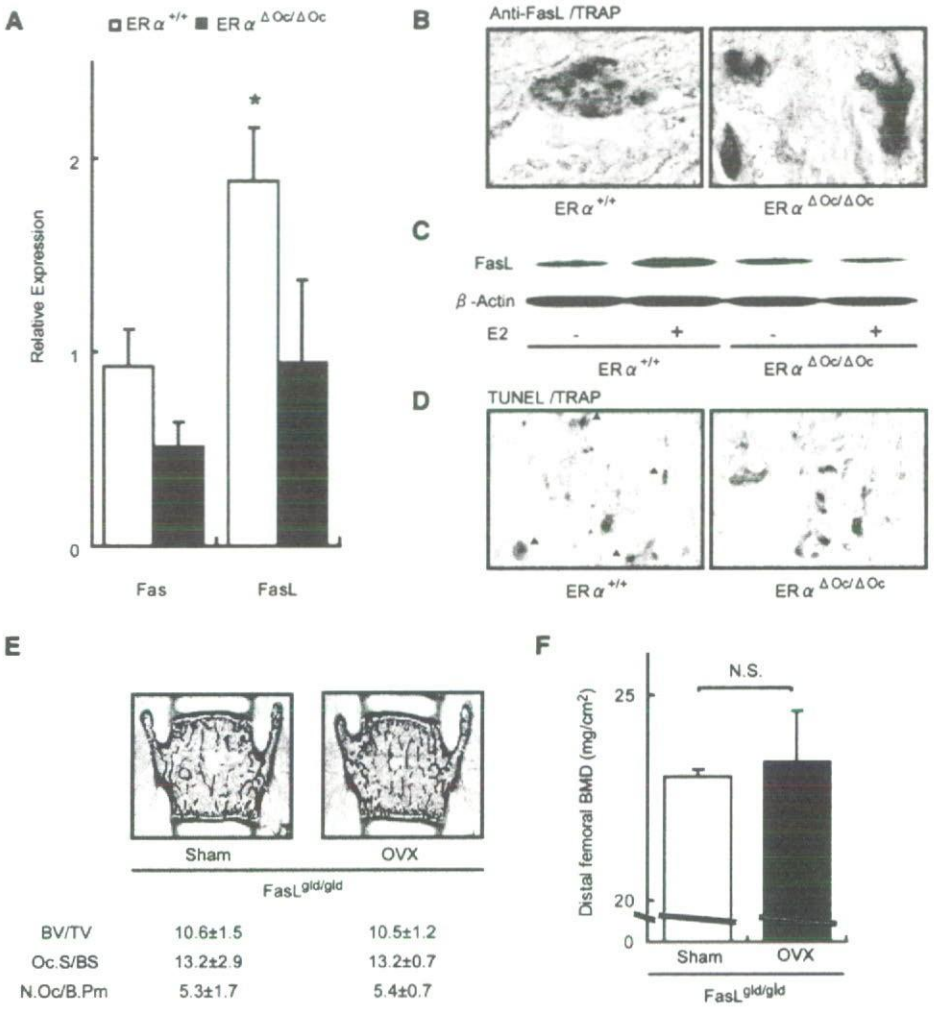

Figure 6. Activated ERα Induced Fas Ligand Expression and Apoptosis in Differentiated Osteoclasts of Intact Bone

(A) Real-time RT-PCR analysis of *Fas* and *FasL*. Expression levels in bones from E2-treated ovariectomized $ER\alpha^{+/+}$ (open column) and $ER\alpha^{\Delta Oc/\Delta Oc}$ (filled column) were compared with the ovariectomized groups of each genotype without E2 administration (*$p < 0.05$ compared to $ER\alpha^{+/+}$). Data are represented as mean ± SEM.

(B) Immunohistochemical analysis of anti-FasL with TRAP staining of the sections from the distal femurs of E2-treated ovariectomized $ER\alpha^{+/+}$ and $ER\alpha^{\Delta Oc/\Delta Oc}$ mice. Brawny stained cells are anti-FasL positive.

(C) Anti-FasL western blot analysis of proteins obtained from femurs of ovariectomized $ER\alpha^{+/+}$ and $ER\alpha^{\Delta Oc/\Delta Oc}$ mice treated with or without E2, using anti-β-actin as internal control.

(D) TUNEL staining with TRAP staining of the sections from the distal femurs of E2-treated ovariectomized $ER\alpha^{+/+}$ and $ER\alpha^{\Delta Oc/\Delta Oc}$ mice. Arrowheads indicate both TUNEL (brown)- and TRAP-positive staining cells.

(E) Bone histomorphometrical analysis of sham-operated or ovariectomized $FasL^{gld/gld}$ mice.

(F) BMD of the distal femurs of sham operated or ovariectomized $FasL^{gld/gld}$ mice. Data are represented as mean ± SEM.

This attenuates bone resorption. This idea is supported by previous observations that estrogen deficiency following menopause or ovariectomy leads to high bone turnover, particularly in the trabecular areas, as bone is rapidly lost through enhanced resorption (Delmas, 2002; Tolar et al., 2004). Thus, estrogen treatment leads to recovery from osteopenia by reducing resorption (Delmas, 2002; Rodan and Martin, 2000), partly by the induction of osteoclast cell death.

In contrast to the osteopenia seen in the $ER\alpha^{\Delta Oc/\Delta Oc}$ females, the $ER\alpha^{\Delta Oc/\Delta Oc}$ male mice unexpectedly had no bone loss. The male mice still demonstrated an ERα-mediated induction of FasL in response to estrogen with subsequent apoptosis of osteoclasts (Figure 7). Both male mice with a deficiency of aromatase that are unable to locally produce estrogen from testosterone and men with a genetic mutation in the *ERα* gene suffer from osteoporosis (Smith et al., 1994). Considering that the

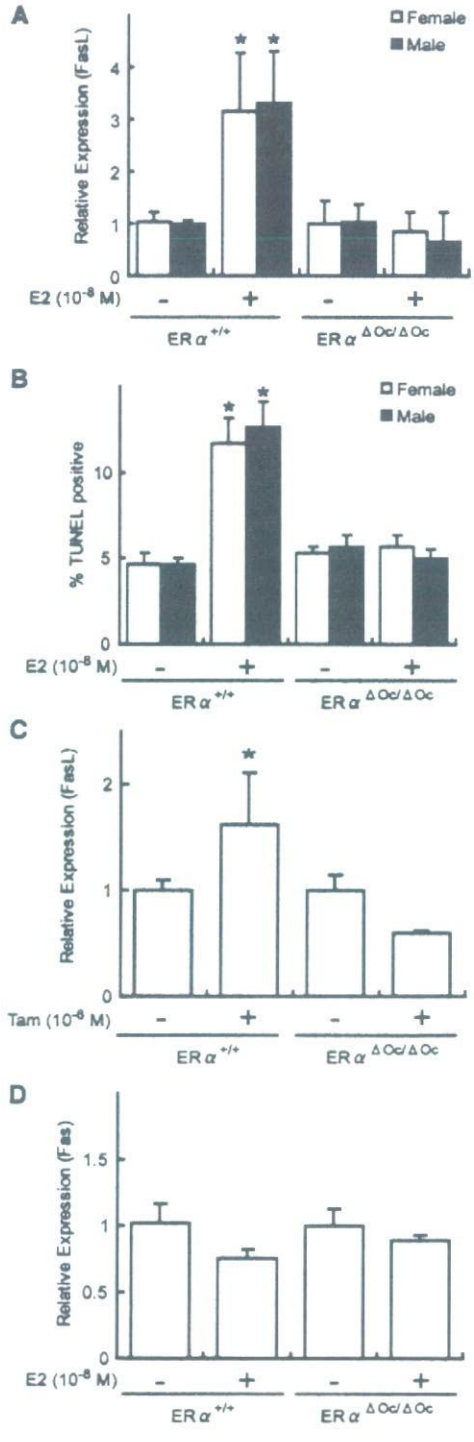

Figure 7. Estrogen-Induced *FasL* Expression and Apoptosis Required ERα in Cultured Osteoclasts

(A) Real-time RT-PCR analysis of *FasL* expression using total RNA obtained from in vitro primary cultured osteoclasts of each genotype at 3 days after RANKL stimulation, treated with or without E2 (10^{-8} M) for 4 hr (*$p < 0.05$ compared to the group treated without E2). Data are represented as mean ± SEM.

(B) Apoptotic cells were defined as those with TUNEL-positive nuclei among TRAP-positive multinucleated primary cultured osteoclasts treated with or without E2 (10^{-8} M) for 12 hr in 96-well plates (*$p < 0.05$ compared to the group treated without E2). Data are represented as mean ± SEM.

(C) *FasL* expression in each genotypic female osteoclastic cells treated with or without Tam (10^{-6} M) (*$p < 0.05$ compared to the group treated without Tam). Data are represented as mean ± SEM.

(D) Expression of *Fas* was measured as described in the legend of Figure 7A. Data are represented as mean ± SEM.

markedly elevated levels of testosterone in ERα KO females may be potent enough to maintain normal bone turnover (Syed and Khosla, 2005), it is likely that the activated AR might be functionally sufficient in male mice to compensate for the ERα deficiency in bone (Kawano et al., 2003). However, species differences in the osteoprotective action of sex steroid hormones still need to be carefully addressed.

Fas/FasL system-mediated apoptotic induction of osteoclasts by estrogen may well be a part of the mechanism for the antiresorptive action of estrogen and SERMs in trabecular bone areas (Delmas, 2002; Rodan and Martin, 2000; Simpson and Davis, 2001; Syed and Khosla, 2005; Tolar et al., 2004). Regulation of osteoclast differentiation is tightly coupled to osteoblastic function in terms of cytokine production and cell-cell contact (Karsenty and Wagner, 2002; Martin and Sims, 2005; Mundy and Elefteriou, 2006; Teitelbaum and Ross, 2003). Indeed, upregulation of osteoclastogenic cytokines by ovariectomy was unaffected in $ER\alpha^{\Delta Oc/\Delta Oc}$ females. Considering the observation that cortical bone mass is increased in ovariectomized $ER\alpha^{\Delta Oc/\Delta Oc}$ females during estrogen treatment, it is conceivable that the antiresorptive estrogen action in cortical bone is also mediated by osteoblastic ERα. In this regard, FasL induction by estrogen in osteoblasts may contribute to the osteoprotective estrogen action, and *FasL* gene induction by estrogen was in fact detected in primary cultured osteoblasts from female calvaria by us as well as another group (S. Krum and M. Brown, personal communication). Thus, similar experiments in which ERα is selectively ablated in osteoblasts are needed to define the role of ERα in these cells.

In osteoclastic cells, expression of the *FasL* gene, which leads to apoptosis, appears to be positive controlled by activated ERα. Not surprisingly, a direct binding site for ERα has been mapped in the *FasL* gene locus (S. Krum and M. Brown, personal communication). An osteoclast- and cell-differentiation stage-specific mechanism may underlie this gene induction in the *FasL* gene promoter. A recent study demonstrated that ERα recruitment to specific promoter sites of given ERα target genes was cell-type specific (Carroll et al., 2005). Thus, there is significant impetus to identify the osteoclastic factor that associates with ERα in the *FasL* gene promoter. Such identification will lead to a better understanding of the molecular basis of the osteoprotective estrogen action and provide a target against which to develop SERMs of greater effectiveness.

EXPERIMENTAL PROCEDURES

Ctsk-Cre Construction and Generation of the Knockin Mouse Lines

An RP23-422n18 BAC clone containing the mouse *Ctsk* gene was purchased from Invitrogen (Carlsbad, CA). The *FRT-Kan^r/Neo^r-FRT* and *nlsCre* fragments were obtained from plasmids pSK2/3-*FRT-Neo* and pIC-*Cre*. Two homologous arms of 500 bp from the *Ctsk* gene were inserted into both sides of the *nlsCre-FRT-Kan^r/Neo^r-FRT* cassette in the pSK2/3-*FRT-Neo* plasmid. The *nlsCre-FRT-Kan^r/Neo^r-FRT* cassette was introduced into the endogenous ATG start site of the *Ctsk* gene by recombineering approaches (Copeland et al., 2001). Targeted BAC was reduced in size from 189 kb to 26 kb and subcloned into the pMC1-DTpA vector by the gap-repair method. The targeted TT2 ES clones were selected after positive-negative selection with G418 and DT-A with Southern analysis, then aggregated with single eight-cell embryos from CD-1 mice (Yoshizawa et al., 1997). Chimeric mice were then crossed with a general deleter mouse line, *ACTB-Flpe* (Jackson Laboratory), to remove the *Kan^r/Neo^r* cassette. The *Ctsk-Cre* mice (*Ctsk$^{Cre/+}$*), originally on a hybrid C57BL/6 and CBA genetic background, were backcrossed for four generations into a C57BL/6J background. *FasL$^{gld/gld}$* mice were also purchased from Jackson Laboratory.

Analysis of Cre Recombinase Activities

Expression of the Cre transcript was detected by RT-PCR. Southern analysis using a *Cre* cDNA probe was performed with total RNA extracted from 12-week-old mice. To evaluate the specificity and efficiency of Cre-mediated recombination, we mated the *Ctsk$^{Cre/+}$* mice to *CAG-CAT-Z* reporter mice (kindly provided by J. Miyazaki) (Sakai and Miyazaki, 1997) and genotyped their offspring with *Cre*-specific primers. β-galactosidase activity of the expressed *LacZ* gene driven by the *CAG* promoter was expected to be detected in the given cells expressing functional Cre recombinase.

In Vitro Osteoclastogenesis and Ligand Application

Bone-marrow cells derived from 8-week-old mice were plated in culture dishes containing α-MEM (GIBCO-BRL) with 10% FBS (JRH) and 10 ng/ml M-CSF (Genzyme). After incubation for 48 hr, adherent cells were used as osteoclast precursor cells after washing out the nonadherent cells. Cells were cultured in the presence of 10 ng/ml M-CSF and 100 ng/ml RANKL (Peprotech) to generate osteoclast-like cells (Koga et al., 2004) for 3 days, so the total culture time was 5 days. Three days after RANKL stimulation, primary cultured osteoclasts were treated with 10^{-8} M of 17β-estradiol (E2) (Sigma-Aldrich Co.) or 10^{-6} M 4-hydroxytamoxifen (Tam) (Sigma-Aldrich Co.) in phenol-red free medium.

Generation of Osteoclast-Specific ERα KO Mice

The ERα conditional (*ERα$^{flox/flox}$*) (Dupont et al., 2000) and null alleles with a C57BL/6J background have been previously described. *ERα$^{flox/flox}$* mice were crossed with *Ctsk$^{Cre/+}$* mice to generate *Ctsk$^{Cre/+}$; ERα$^{flox/+}$* mice. *Ctsk$^{Cre/+}$; ERα$^{+/+}$* (*ERα$^{+/+}$*) and *Ctsk$^{Cre/+}$; ERα$^{flox/flox}$* (*ERα$^{\Delta Oc/\Delta Oc}$*) mice were obtained by crossing *Ctsk$^{Cre/+}$; ERα$^{flox/+}$* with *ERα$^{flox/+}$* mouse lines.

Radiological Analysis

Bone radiographs of the femurs of 12-week-old *Ctsk$^{Cre/+}$; ERα$^{flox/flox}$* (*ERα$^{\Delta Oc/\Delta Oc}$*) and *Ctsk$^{Cre/+}$; ERα$^{+/+}$* (*ERα$^{+/+}$*) littermates were visualized with a soft X-ray apparatus (TRS-1005: SOFTRON). BMD was measured by DXA using a bone mineral analyzer (DCS-600EX: ALOKA). Micro Computed Tomography scanning of the femurs was performed using a composite X-ray analyzer (NX-CP-C80H-IL: Nittetsu ELEX Co.) (Kawano et al., 2003). Tomograms were obtained with a slice thickness of 10 μm and reconstructed at 12 × 12 pixels into a 3D image by the volume-rending method (VIP-Station; Teijin System Technology) using a computer.

Analysis of Skeletal Morphology

Twelve-week-old *Ctsk$^{Cre/+}$; ERα$^{flox/flox}$* (*ERα$^{\Delta Oc/\Delta Oc}$*) and *Ctsk$^{Cre/+}$; ERα$^{+/+}$* (*ERα$^{+/+}$*) littermates were double labeled with subcutaneous injections of 16 mg/kg of calcein (Sigma) at 4 and 2 days before sacrifice. Tibiae were removed from each mouse and fixed with 70% ethanol. They were stained with Villanueva bone stain for 7 days and embedded in methyl-methacrylate (Wako) (Yoshizawa et al., 1997). Frontal plane sections (5-μm thick) of the proximal tibia were cut using a Microtome (LEICA). The cancellous bone was measured in the secondary spongiosa located 500 μm from the epiphyseal growth plate and 160 μm from the endocortical surface (Kawano et al., 2003; Nakamichi et al., 2003). Bone histomorphometric measurements of the tibia were made using a semiautomatic image analyzing system (System Supply) and a fluorescent microscope (Optiphot; Nikon). Similar measurements of the lumbar vertebral bodies were done as previously reported (Takeda et al., 2002). Standard bone histomorphometrical nomenclatures, symbols, and units were used as described in the report of the ASBMR Histomophometry Nomenclature Committee.

Ovariectomy and Hormone Replacement

Female *Ctsk$^{Cre/+}$; ERα$^{flox/flox}$* (*ERα$^{\Delta Oc/\Delta Oc}$*) and *Ctsk$^{Cre/+}$; ERα$^{+/+}$* (*ERα$^{+/+}$*) littermates were ovariectomized or sham operated at 8–12 weeks of age for 2 weeks for all experiments, and slow releasing pellets of E2 (0.83 μg/day) or placebo (Innovative Research, Sarasota, FL) were implanted subcutaneously in the scapular region behind the neck (Sato et al., 2004; Shiina et al., 2006).

Immunohistochemistry

Twelve-week-old *Ctsk$^{Cre/+}$; ERα$^{flox/flox}$* (*ERα$^{\Delta Oc/\Delta Oc}$*) and *Ctsk$^{Cre/+}$; ERα$^{+/+}$* (*ERα$^{+/+}$*) littermates were fixed with 4% PFA by perfusion. Serial sections of the brain (20 μm thick) were divided into two groups and used for single labeling for the ERα or thionin to allow determination of the areas to be measured. Tibiae and femurs were decalcified in 10% EDTA for 2–4 weeks after fixation and then embedded in paraffin sections. Sections were incubated in L.A.B. solution (Polysciences) for 30 min to retrieve antigen. The cooled sections were incubated in 1% H_2O_2 for 30 min to quench endogenous peroxidase and then washed with 1% Triton X-100 in PBS for 10 min. To block nonspecific antibody binding, sections were incubated in blocking solution (DAKO) for 5 min. Sections were then incubated with anti-ERα (Santa Cruz, CA) and anti-FasL (Santa Cruz, CA) in blocking solution overnight at 4°C. Staining was then performed using the EnVision+ HRP System (Dako) and 3, 3′-diaminobendizine tetrahydrochloride substrate (Sigma), counterstained with TRAP, dehydrated through an ethanol series and xylene, before mounting (Sato et al., 2004).

ERα Overexpression

Two days after RANKL stimulation, an expression vector of mouse ERα was tranfected into immature osteoclastic cells from *ERα$^{\Delta Oc/\Delta Oc}$* mice using Superfect (QIAGEN) as manufacture's instruction.

Real-Time RT-PCR

One microgram of total RNA from each sample was reverse transcribed into first-strand cDNA with random hexamers using Superscript III reverse transcriptase (Invitrogen). Primer sets for all genes were purchased from Takara Bio. Inc. (Tokyo, Japan). Real-time RT-PCR was performed using SYBR Premix Ex Taq (Takara) with the ABI PRISM 7900HT (Applied Biosystems) according to the manufacturer's instructions. Experimental samples were matched to a standard curve generated by amplifying serially diluted products using the same PCR protocol. To correct for variability in RNA recovery and efficiency of reverse transcription, *Gapdh* cDNA was amplified and quantified in each cDNA preparation. Normalization and calculation steps were performed as reported previously (Takezawa et al., 2007).

TUNEL/TRAP Staining

The TUNEL method was performed using the ApopTag Fluorescein In Situ Apoptosis Detection Kit (CHEMICON international) according to the manufacturer's instructions with a slight modification. This was followed by TRAP staining as previously reported (**Kobayashi et al., 2000**).

Cytokine Assays

Bone marrow and blood were collected at 2 weeks after sham operation or ovariectomy. Bone-marrow cells were cultured for 3 days in DMEM. The levels of TNFα, IL-1α, and IL-6 in the culture media and serum RANKL were determined by ELISA (R&D Systems).

Western Blot

Osteoclast precursor cells were treated with or without 100 ng/ml of soluble RANKL. After 15 minutes, cell extracts were harvested from the cells using lysis buffer containing 100 mM Tris-HCl (pH 7.8), 150 mM NaCl, 0.1% Triton X-100, 5% protease inhibitor cocktail (Sigma), and 5% phosphatase inhibitor cocktail (Sigma). An equivalent amount of protein from each of the cell extracts and proteins of femoral bone extracted using ISOGEN was loaded for SDS-PAGE and transferred to PVDF membranes (Amersham Biosciences). The membranes were developed with enhanced chemiluminescence reagent (Amersham Biosciences) (**Ohtake et al., 2003**). Phosphorylation of p38 MAPK and IκB were evaluated using antibodies purchased from Cell Signaling Technology (**Koga et al., 2004**) and anti-FasL antibody was purchased from Santa Cruz Biotechnology (sc-834).

Actin-Ring Formation

Cells were fixed for 15 min in warm 4% paraformaldehyde (PFA). After fixation, cells were washed three times with PBS with 0.1% Triton X-100 (PBST) and incubated with 0.2 U/ml rhodamine phalloidin (Molecular Probes) for 30 min and washed again three times in PBST.

Statistical Analysis

Data were analyzed by two-tailed student's t test. For all graphs, data are represented as mean ± SEM.

Supplemental Data

Supplemental Data include Supplemental Experimental Procedures and four figures and can be found with this article online at http://www.cell.com/cgi/content/full/130/5/811/DC1/.

ACKNOWLEDGMENTS

We thank Drs. S. Krum and M. Brown to share with their unpublished results; Drs. K. Yoshimura, Y. Nakamichi, T. Watanabe, J. Miyamoto, H. Shiina, T. Fukuda, Ms. Y. Sato, and S. Tanaka for generation of the KO mice; Drs. T. Koga, H. Takagi, E. Ochiai, and N. Moriyama for technical help; Dr. J. Miyazaki for *CAG-CAT-Z* reporter mice, and H. Higuchi and K. Hiraga for manuscript preparation. This work was supported in part by priority areas from the Ministry of Education, Culture, Sports, Science and Technology (to S.K.) and the Program for Promotion of Basic Research Activities for Innovative Biosciences (PROBRAIN).

Received: February 23, 2007
Revised: May 21, 2007
Accepted: July 17, 2007
Published: September 6, 2007

REFERENCES

Belandia, B., and Parker, M.G. (2003). Nuclear receptors: a rendezvous for chromatin remodeling factors. Cell *114*, 277–280.

Bland, R. (2000). Steroid hormone receptor expression and action in bone. Clin. Sci. (Lond.) *98*, 217–240.

Carroll, J.S., Liu, X.S., Brodsky, A.S., Li, W., Meyer, C.A., Szary, A.J., Eeckhoute, J., Shao, W., Hestermann, E.V., Geistlinger, T.R., et al. (2005). Chromosome-wide mapping of estrogen receptor binding reveals long-range regulation requiring the forkhead protein FoxA1. Cell *122*, 33–43.

Chien, K.R., and Karsenty, G. (2005). Longevity and lineages: toward the integrative biology of degenerative diseases in heart, muscle, and bone. Cell *120*, 533–544.

Copeland, N.G., Jenkins, N.A., and Court, D.L. (2001). Recombineering: a powerful new tool for mouse functional genomics. Nat. Rev. Genet. *2*, 769–779.

Couse, J.F., and Korach, K.S. (1999). Estrogen receptor null mice: what have we learned and where will they lead us? Endocr. Rev. *20*, 358–417.

Delmas, P.D. (2002). Treatment of postmenopausal osteoporosis. Lancet *359*, 2018–2026.

Dupont, S., Krust, A., Gansmuller, A., Dierich, A., Chambon, P., and Mark, M. (2000). Effect of single and compound knockouts of estrogen receptors alpha (ERalpha) and beta (ERbeta) on mouse reproductive phenotypes. Development *127*, 4277–4291.

Gowen, M., Lazner, F., Dodds, R., Kapadia, R., Feild, J., Tavaria, M., Bertoncello, I., Drake, F., Zavarselk, S., Tellis, I., et al. (1999). Cathepsin K knockout mice develop osteopetrosis due to a deficit in matrix degradation but not demineralization. J. Bone Miner. Res. *14*, 1654–1663.

Harada, S., and Rodan, G.A. (2003). Control of osteoblast function and regulation of bone mass. Nature *423*, 349–355.

Kameda, T., Mano, H., Yuasa, T., Mori, Y., Miyazawa, K., Shiokawa, M., Nakamaru, Y., Hiroi, E., Hiura, K., Kameda, A., et al. (1997). Estrogen inhibits bone resorption by directly inducing apoptosis of the bone-resorbing osteoclasts. J. Exp. Med. *186*, 489–495.

Karsenty, G. (2006). Convergence between bone and energy homeostases: leptin regulation of bone mass. Cell Metab. *4*, 341–348.

Karsenty, G., and Wagner, E.F. (2002). Reaching a genetic and molecular understanding of skeletal development. Dev. Cell *2*, 389–406.

Kato, S., Ito, S., Noguchi, T., and Naito, H. (1989). Effects of brefeldin A on the synthesis and secretion of egg white proteins in primary cultured oviduct cells of laying Japanese quail (Coturnix coturnix japonica). Biochim. Biophys. Acta *991*, 36–43.

Kawano, H., Sato, T., Yamada, T., Matsumoto, T., Sekine, K., Watanabe, T., Nakamura, T., Fukuda, T., Yoshimura, K., Yoshizawa, T., et al. (2003). Suppressive function of androgen receptor in bone resorption. Proc. Natl. Acad. Sci. USA *100*, 9416–9421.

Kimble, R.B., Matayoshi, A.B., Vannice, J.L., Kung, V.T., Williams, C., and Pacifici, R. (1995). Simultaneous block of interleukin-1 and tumor necrosis factor is required to completely prevent bone loss in the early postovariectomy period. Endocrinology *136*, 3054–3061.

Kobayashi, Y., Hashimoto, F., Miyamoto, H., Kanaoka, K., Miyazaki-Kawashita, Y., Nakashima, T., Shibata, M., Kobayashi, K., Kato, Y., and Sakai, H. (2000). Force-induced osteoclast apoptosis in vivo is accompanied by elevation in transforming growth factor beta and osteoprotegerin expression. J. Bone Miner. Res. *15*, 1924–1934.

Koga, T., Inui, M., Inoue, K., Kim, S., Suematsu, A., Kobayashi, E., Iwata, T., Ohnishi, H., Matozaki, T., Kodama, T., et al. (2004). Costimulatory signals mediated by the ITAM motif cooperate with RANKL for bone homeostasis. Nature *428*, 758–763.

Li, C.Y., Jepsen, K.J., Majeska, R.J., Zhang, J., Ni, R., Gelb, B.D., and Schaffler, M.B. (2006). Mice lacking Cathepsin K maintain bone remodeling but develop bone fragility despite high bone mass. J. Bone Miner. Res. *21*, 865–875.

Mangelsdorf, D.J., Thummel, C., Beato, M., Herrlich, P., Schutz, G., Umesono, K., Blumberg, B., Kastner, P., Mark, M., Chambon, P., and Evans, R.M. (1995). The nuclear receptor superfamily: the second decade. Cell *83*, 835–839.

Martin, T.J., and Sims, N.A. (2005). Osteoclast-derived activity in the coupling of bone formation to resorption. Trends Mol. Med. *11*, 76–81.

Mueller, S.O., and Korach, K.S. (2001). Estrogen receptors and endocrine diseases: lessons from estrogen receptor knockout mice. Curr. Opin. Pharmacol. *1*, 613–619.

Mundy, G.R., and Elefteriou, F. (2006). Boning up on ephrin signaling. Cell *126*, 441–443.

Nakamichi, Y., Shukunami, C., Yamada, T., Aihara, K., Kawano, H., Sato, T., Nishizaki, Y., Yamamoto, Y., Shindo, M., Yoshimura, K., et al. (2003). Chondromodulin I is a bone remodeling factor. Mol. Cell. Biol. *23*, 636–644.

Ohtake, F., Takeyama, K., Matsumoto, T., Kitagawa, H., Yamamoto, Y., Nohara, K., Tohyama, C., Krust, A., Mimura, J., Chambon, P., et al. (2003). Modulation of oestrogen receptor signalling by association with the activated dioxin receptor. Nature *423*, 545–550.

Raisz, L.G. (2005). Pathogenesis of osteoporosis: concepts, conflicts, and prospects. J. Clin. Invest. *115*, 3318–3325.

Riggs, B.L., and Hartmann, L.C. (2003). Selective estrogen-receptor modulators–mechanisms of action and application to clinical practice. N. Engl. J. Med. *348*, 618–629.

Rodan, G.A., and Martin, T.J. (2000). Therapeutic approaches to bone diseases. Science *289*, 1508–1514.

Saftig, P., Hunziker, E., Wehmeyer, O., Jones, S., Boyde, A., Rommerskirch, W., Moritz, J.D., Schu, P., and von Figura, K. (1998). Impaired osteoclastic bone resorption leads to osteopetrosis in Cathepsin-K-deficient mice. Proc. Natl. Acad. Sci. USA *95*, 13453–13458.

Sakai, K., and Miyazaki, J. (1997). A transgenic mouse line that retains Cre recombinase activity in mature oocytes irrespective of the cre transgene transmission. Biochem. Biophys. Res. Commun. *237*, 318–324.

Sato, T., Matsumoto, T., Kawano, H., Watanabe, T., Uematsu, Y., Sekine, K., Fukuda, T., Aihara, K., Krust, A., Yamada, T., et al. (2004). Brain masculinization requires androgen receptor function. Proc. Natl. Acad. Sci. USA *101*, 1673–1678.

Shang, Y., and Brown, M. (2002). Molecular determinants for the tissue specificity of SERMs. Science *295*, 2465–2468.

Shiina, H., Matsumoto, T., Sato, T., Igarashi, K., Miyamoto, J., Takemasa, S., Sakari, M., Takada, I., Nakamura, T., Metzger, D., et al. (2006). Premature ovarian failure in androgen receptor-deficient mice. Proc. Natl. Acad. Sci. USA *103*, 224–229.

Simpson, E.R., and Davis, S.R. (2001). Minireview: aromatase and the regulation of estrogen biosynthesis–some new perspectives. Endocrinology *142*, 4589–4594.

Sims, N.A., Clement-Lacroix, P., Minet, D., Fraslon-Vanhulle, C., Gaillard-Kelly, M., Resche-Rigon, M., and Baron, R. (2003). A functional androgen receptor is not sufficient to allow estradiol to protect bone after gonadectomy in estradiol receptor-deficient mice. J. Clin. Invest. *111*, 1319–1327.

Smith, E.P., Boyd, J., Frank, G.R., Takahashi, H., Cohen, R.M., Specker, B., Williams, T.C., Lubahn, D.B., and Korach, K.S. (1994). Estrogen resistance caused by a mutation in the estrogen-receptor gene in a man. N. Engl. J. Med. *331*, 1056–1061.

Sun, L., Peng, Y., Sharrow, A.C., Iqbal, J., Zhang, Z., Papachristou, D.J., Zaidi, S., Zhu, L.L., Yaroslavskiy, B.B., Zhou, H., et al. (2006). FSH directly regulates bone mass. Cell *125*, 247–260.

Suzawa, M., Takada, I., Yanagisawa, J., Ohtake, F., Ogawa, S., Yamauchi, T., Kadowaki, T., Takeuchi, Y., Shibuya, H., Gotoh, Y., et al. (2003). Cytokines suppress adipogenesis and PPAR-gamma function through the TAK1/TAB1/NIK cascade. Nat. Cell Biol. *5*, 224–230.

Syed, F., and Khosla, S. (2005). Mechanisms of sex steroid effects on bone. Biochem. Biophys. Res. Commun. *328*, 688–696.

Takeda, S., Elefteriou, F., Levasseur, R., Liu, X., Zhao, L., Parker, K.L., Armstrong, D., Ducy, P., and Karsenty, G. (2002). Leptin regulates bone formation via the sympathetic nervous system. Cell *111*, 305–317.

Takezawa, S., Yokoyama, A., Okada, M., Fujiki, R., Iriyama, A., Yanagi, Y., Ito, H., Takada, I., Kishimoto, M., Miyajima, A., et al. (2007). A cell cycle-dependent co-repressor mediates photoreceptor cell-specific nuclear receptor function. EMBO J. *26*, 764–774.

Teitelbaum, S.L. (2006). Osteoclasts; culprits in inflammatory osteolysis. Arthritis Res. Ther. *8*, 201.

Teitelbaum, S.L. (2007). Osteoclasts: what do they do and how do they do it? Am. J. Pathol. *170*, 427–435.

Teitelbaum, S.L., and Ross, F.P. (2003). Genetic regulation of osteoclast development and function. Nat. Rev. Genet. *4*, 638–649.

Tolar, J., Teitelbaum, S.L., and Orchard, P.J. (2004). Osteopetrosis. N. Engl. J. Med. *351*, 2839–2849.

Windahl, S.H., Andersson, G., and Gustafsson, J.A. (2002). Elucidation of estrogen receptor function in bone with the use of mouse models. Trends Endocrinol. Metab. *13*, 195–200.

Yoshizawa, T., Handa, Y., Uematsu, Y., Takeda, S., Sekine, K., Yoshihara, Y., Kawakami, T., Arioka, K., Sato, H., Uchiyama, Y., et al. (1997). Mice lacking the vitamin D receptor exhibit impaired bone formation, uterine hypoplasia and growth retardation after weaning. Nat. Genet. *16*, 391–396.

Zaman, G., Jessop, H.L., Muzylak, M., De Souza, R.L., Pitsillides, A.A., Price, J.S., and Lanyon, L.L. (2006). Osteocytes use estrogen receptor alpha to respond to strain but their ERalpha content is regulated by estrogen. J. Bone Miner. Res. *21*, 1297–1306.

Accession Numbers

Microarray can be seen in Gene Expression Omnibus under accession number GSE7798.

Fish Oil Prevents Sucrose-Induced Fatty Liver But Exacerbates High-Safflower Oil-Induced Fatty Liver in ddY Mice

Tomomi Yamazaki, Akiko Nakamori, Eriko Sasaki, Satoshi Wada, and Osamu Ezaki

Diets high in sucrose/fructose or fat can result in hepatic steatosis (fatty liver). We analyzed the effects of dietary fish oil on fatty liver induced by sucrose, safflower oil, and butter in ddY mice. In experiment I, mice were fed a high-starch diet [70 energy% (en%) starch] plus 20% (wt/wt) sucrose in the drinking water or fed a high-safflower oil diet (60 en%) for 11 weeks. As a control, mice were fed a high-starch diet with drinking water. Fish oil (10 en%) was either supplemented or not. Mice supplemented with sucrose or fed safflower oil showed a 1.7-fold or 2.2-fold increased liver triglyceride content, respectively, compared with that of control mice. Fish oil completely prevented sucrose-induced fatty liver, whereas it exacerbated safflower oil-induced fatty liver. Sucrose increased SREBP-1c and target gene messenger RNAs (mRNAs), and fish oil completely inhibited these increases. In experiment II, mice were fed a high-safflower oil or a high-butter diet, with or without fish oil supplementation. Fish oil exacerbated safflower oil–induced fatty liver but did not affect butter-induced fatty liver. Fish oil increased expression of peroxisome proliferator-activated receptor gamma (PPARγ) and target CD36 mRNA in safflower oil-fed mice. These increases were not observed in sucrose-supplemented or butter-fed mice. *Conclusion:* The effects of dietary fish oil on fatty liver differ according to the cause of fatty liver; fish oil prevents sucrose-induced fatty liver but exacerbates safflower oil-induced fatty liver. The exacerbation of fatty liver may be due, at least in part, to increased expression of liver PPARγ.
(HEPATOLOGY 2007;46:1779-1790.)

The prevalence of obesity in Western societies has increased dramatically, due in large part to high-fat (HF) and high-sucrose diets. Among the consequences of obesity are the emerging epidemics of hepatic steatosis and nonalcoholic fatty liver disease (NAFLD). NAFLD occurs in patients who consume little or no alcohol.[1] Fatty liver has been thought to be benign. However, it is now understood that fatty liver is a precursor of nonalcoholic steatohepatitis, which progresses to cirrhosis in up to 25% of patients.[2]

The accumulated hepatic lipids in patients with NAFLD include plasma nonesterified fatty acids (NEFAs) from adipose tissue, fatty acids produced in the liver via *de novo* lipogenesis, and dietary fatty acids, which enter the liver via spillover into the plasma NEFA pool and via hepatic uptake of intestinally derived chylomicron remnants. Analysis of multiple stable isotopes in patients with NAFLD has revealed that, of the triglyceride (TG) in the liver, 59% is derived from NEFAs, 26% from *de novo* lipogenesis, and 15% from dietary fatty acids.[3] Roughly one fourth of fatty acids in the liver is produced from *de novo* 2-carbon precursors derived from glucose, fructose, and amino acids. Dietary fat also contributes significantly to liver TG storage pools.

Abbreviations: ACC, acetyl-CoA carboxylase; ACO, acyl-CoA oxidase; ANOVA, analysis of variance; CD36, fatty acid translocase; ChREBP, carbohydrate response element-binding protein; CPT, carnitine palmitoyltransferase; CREB, cAMP response element-binding protein; DGAT, acyl-CoA:diacylglycerol acyltransferase; DHA, docosahexaenoic acid; en%, energy percent; EPA, eicosapentaenoic acid; FAS, fatty acid synthase; GPAT, acyl-CoA:glycerol-3-phosphate acyltransferase; HF, high-fat; LPK, liver-type pyruvate kinase; LXR, liver X receptor; MCAD, medium-chain acyl-CoA dehydrogenase; mRNA, messenger RNA; NAFLD, nonalcoholic fatty liver disease; NEFA, nonesterified fatty acid; PCR, polymerase chain reaction; PGC, peroxisome proliferator-activated receptor r coactivator; PPAR, peroxisome proliferator-activated receptor; QUICKI, quantitive insulin sensitivity check index; SCD, stearoyl-CoA desaturase; SREBP, sterol regulatory element-binding protein; WAT, white adipose tissue; TG, triglyceride.

From the Nutritional Science Program, National Institute of Health and Nutrition, Tokyo, Japan.

Received January 16, 2007; accepted July 18, 2007.

Supported in part by a grant-in-aid for scientific research Kakenhi from the Japanese Ministry of Education, Culture, Sports, Science and Technology (MEXT, Tokyo, Japan), by research grants from the Japanese Ministry of Health, Labour and Welfare, by a grant-in-aid for the Development of Evaluation and Management Methods for Supply of Safe, Reliable and Functional Food and Farm Produce from the Japanese Ministry of Agriculture, Forestry and Fisheries, and by a grant for the Promotion of Fundamental Studies in Health Sciences from the Organization for Pharmaceutical Safety and Research (OPSR, Osaka, Japan).

Address reprint requests to: Tomomi Yamazaki, Ph.D., or Osamu Ezaki, M.D., Nutritional Science Program, National Institute of Health and Nutrition, 1-23-1, Toyama, Shinjuku-ku, Tokyo 162-8636, Japan. E-mail: tomo0322@nih.go.jp or ezaki@nih.go.jp; fax: 81-3-3207-3520.

Published online in Wiley InterScience (www.interscience.wiley.com).

DOI 10.1002/hep.21934

Potential conflict of interest: Nothing to report.

Table 1. Dietary Composition in Experiments I and II

Ingredients	St	St+FO	Suc	Suc+FO	Saf	Saf+FO	Butter	Butter+FO
				g/100g				
Safflower oil	4.0	-	4.0	-	33.5	29.5	-	-
Butter	-	-	-	-	-	-	33.5	29.5
Fish oil	-	4.0	-	4.0	-	4.0	-	4.0
Casein	20.0	20.0	20.0	20.0	29.0	29.0	29.0	29.0
Sucrose	-	-	-	-	23.3	23.3	23.3	23.3
α-Starch	66.2	66.2	66.2	66.2	-	-	-	-
Vitamin mix (AIN-93)	1.0	1.0	1.0	1.0	1.5	1.5	1.5	1.5
Mineral mix (AIN-93)	3.5	3.5	3.5	3.5	5.1	5.1	5.1	5.1
Cellulose powder	5.0	5.0	5.0	5.0	7.3	7.3	7.3	7.3
L-cysteine	0.3	0.3	0.3	0.3	0.4	0.4	0.4	0.4

Abbreviations: St, high-starch diet; St+FO, high-starch diet plus fish oil supplementation; Suc, high-starch diet with 20% (w/w) sucrose drink; Suc+FO, high-starch diet with 20% (w/w) sucrose drink plus fish oil supplementation; Saf, high-safflower oil, Saf+FO, high safflower oil plus fish oil supplementation; Butter, high-butter; Butter+FO, high butter plus fish oil supplementation.

Fish oil contains n-3 fatty acids such as eicosapentaenoic acid (EPA) and docosahexaenoic acid (DHA), which, when included in the diet, decrease blood TG concentrations in hypertriglycemic patients and are considered to have protective effects against fatty liver.[4] This effect is attributable mainly to the combined effects of inhibition of lipogenesis and stimulation of fatty acid oxidation in the liver.[5,6] Fish oil supplementation may be effective in the prevention of NAFLD; however, it is not clear whether fish oil is effective against all types of fatty liver.

The C57BL/6J inbred mouse strain has been used for studies of obesity and diabetes because of its susceptibility to these diseases in response to an HF diet.[6,7] C57BL/6J mice also develop fatty liver in response to an HF diet.[8-10] However, they are resistant to sucrose/fructose–induced fatty liver because they possess adenine −468 bp from the putative 5′ end of the sterol regulatory element-binding protein (SREBP)-1c gene.[11] Mice with guanine at this site show increased liver SREBP-1c messenger RNA (mRNA) in response to a high-fructose diet, whereas mice with adenine do not.[11] It has been reported that ddY mice show increased body weight and liver weight in response to 20% sucrose supplementation.[12] We found that ddY mice possess guanine −468 bp in the *SREBP-1c* promoter and show hepatic steatosis when fed either sucrose supplementation or an HF diet (Yamazaki et al., unpublished observation).

In this study, we used ddY mice to examine whether fish oil can prevent fatty liver induced by sucrose supplementation or 2 types of HF diet (safflower oil or butter), and the mechanisms involved were elucidated.

Materials and Methods

Animals. Six-week-old male ddY mice were obtained from Japan SLC Inc. (Hamamatsu, Japan) and fed a normal laboratory diet (CE2; Clea, Tokyo, Japan) for 1 week to stabilize metabolic conditions. Mice were exposed to a 12-hour light/12-hour dark cycle, and the room was maintained at a constant temperature of 22°C. All animal procedures were in accordance with institutional guidelines.

Diet. At 7 weeks of age, ddY mice were assigned to 1 of 6 groups (n = 5-9 in each group). In experiment I, to investigate fatty liver induced by sucrose or high-safflower oil, 3 groups were created: control mice were fed a high-starch diet containing 70 energy% (en%) starch and 10 en% safflower oil, sucrose-supplemented mice were fed a high-starch diet plus 20% sucrose (wt/wt) in the drinking water, and high-safflower oil-fed mice were given 20 en% sucrose plus 60 en% safflower oil. In the HF diet, to promote fat consumption, sucrose rather than starch was used as the carbohydrate source. Control and HF diet-fed mice were given distilled water. In experiment II, to investigate fatty liver induced by high-safflower oil and high-butter, 3 groups were created: control mice were fed a high-starch diet, high-safflower oil-fed mice were given 60 en% safflower oil, and high-butter-fed mice were given 60 en% butter. To examine the effects of fish oil, 10 en% safflower oil or butter was replaced with 10 en% fish oil in experiments I and II. Duration of the dietary manipulation was 11 weeks. The detailed compositions of the experimental diets are listed in Table 1. Fatty acid compositions of dietary oils were measured by gas–liquid chromatography. Safflower oil (high-oleic type) contained 45% oleic acid (18:1n-9) and 46% linoleic acid (18:2n-6), fish oil from tuna contained 7% EPA (20:5n-3) and 24% DHA (22:6n-3), and butter contained 71% (wt:wt) saturated fatty acid including 45% palmitic acid (16:0), 11% stearic acid (18:0), and 22% oleic acid. Diet preparations were similar to those of our previous studies.[5,6] Fish oil was provided by NOF Corp. (Tokyo, Japan). Butter was purchased from Snow Brand Milk Corp. (Hokkaido, Japan).

Table 2. Primers Used for Quantitative PCR

Gene	Forward primer (5′ to 3′)	Reverse primer (5′ to 3′)
ACC1	GGACAGACTGATCGCAGAGAAAG	TGGAGAGCCCCACACACA
ACO	GCCCAACTGTGACTTCCATT	GGCATGTAACCCGTAGCACT
CD36	AATGGCACAGACGCAGCCT	GGTTGTCTGGATTCTGGA
ChREBP	GATGGTGCGAACAGCTCTTCT	CTGGGCTGTGTCATGGTGAA
CPT I	GCACTGCAGCTCGCACATTACAA	CTCAGACAGTACCTCCTTCAGGAAA
CREB	GAAGAAGCAGCACGGAAGAGA	TCTCTTGCTGCCTCCCTGTT
DGAT1	GTGCACAAGTGGTGCATCAG	CAGTGGGATCTGAGCCATC
DGAT2	AGTGGCAATGCTATCATCATCGT	AAGGAATAAGTGGGAACCAGATCA
FAS	GCTGCGGAAACTTCAGGAAAT	AGAGACGTGTCACTCCTGGACTT
GPAT	CAACACCATCCCCGACATC	GTGACCTTCGATTATGCGATCA
HES-1	CACGACACCGGACAAACCA	TCCATGATAGGCTTTGATGACTTTC
LPK	GAGTCGGAGGTGGAAATTGT	CCGCACCACTAAGGAGATGA
LXRα	GGGAGGAGTGTGTCCTGTCAG	GAGCGCCTGTTACACTGTTGC
MCAD	GATCGCAATGGGTGCTTTTGATAGAA	AGCTGATTGGCAATGTCTCCAGCAAA
PGC1β	GGTCCCTGGCTGACATTCAC	GGCACATCGAGGGCAGAG
PPARα	CCTGAACATCGAGTGTCGAATAT	GGTCTTCTTCTGAATCTTGCAGCT
PPARγ1	GAGTGTGACGACAAGATTTG	GGTGGGCCAGAATGGCATCT
PPARγ2	TCTGGGAGATTCTCCTGTTGA	GGTGGGCCAGAATGGCATCT
SCD1	CCCCTGCGGATCTTCCTTAT	AGGGTCGGCGTGTGTTTCT
SREBP-1a	GAGGCGGCTCTGGAACAGA	TGTCTTCGATGTCGTTCAAAACC
SREBP-1c	GGAGCCATGGATTGCACATT	CCTGTCTCACCCCCAGCATA

Consumption of food was measured daily. Drinking of sucrose water was measured weekly. The mean food intake per day was estimated by subtracting the food weight of that day from the initial food weight of the previous day and dividing by the number of mice housed in the cage. With the use of these data, average energy intakes were estimated.

Quantitative Reverse Transcription Polymerase Chain Reaction. Mice were killed, and livers were isolated for RNA preparation in the morning from 3-hour fasted animals to avoid acute effects of food intake. RNA was extracted with TRIzol Reagent (Invitrogen Corp., Carlsbad, CA) according to the manufacturer's instructions. Total RNA isolated from liver was reverse transcribed with ReverTra Ace (Toyobo Co. Ltd., Osaka, Japan) with random hexamers. The resulting complementary DNA was polymerase chain reaction (PCR) amplified in the 96-well format with SYBR Green PCR Master Mix and a 7500 Real-Time PCR System (Applied Biosystems, Foster City, CA). Expression levels of test genes were normalized to those of an endogenous control, acidic ribosomal phosphoprotein P0 (36B4). The primers used for quantitative reverse transcription PCR are listed in Table 2.

Liver Lipid Analysis. Liver lipids were measured by enzymatic colorimetry as described previously.[13]

Serum Chemistries. In experiment II, serum was obtained at 2 points, after 24 hours of fasting and 3 hours after refeeding (postprandial). Serum glucose was measured on an Ascensia autoanalyzer (Bayer Medical Ltd., Tokyo, Japan). Serum TG and NEFA levels were assayed by enzymatic colorimetry with TG E and NEFA C test kits (Wako Pure Chemical Industries Ltd., Osaka, Japan). Serum insulin was determined with a mouse insulin enzyme-linked immunosorbent assay kit (Morinaga, Kanagawa, Japan).

Hepatic Histology. In experiment I, mouse livers were fixed in 4% neutral-buffered formalin, embedded in paraffin, cut into sections, and stained with hematoxylin-eosin. Frozen sections of formalin-fixed liver were stained with Oil red O with the use of standard techniques.

Statistical Analysis. Two-way analysis of variance (ANOVA) was used to examine the 2 main effects of diet (starch, sucrose, and safflower oil) or fat (safflower oil and butter), fish oil supplementation, and their interaction. Statistical significance of the interaction of diet (or fat) and fish oil indicates that the effects of fish oil on the 3 types of diet (or 2 types of fat) were statistically different. When differences were significant with respect to main or interaction effects, each group was compared with the others by Fisher's protected least significant difference test (StatView 5.0; Abacus Concepts Inc., Berkeley, CA). Statistical significance was set at $P < 0.05$. Values are shown as mean ± standard error of the mean (SEM).

Results

Energy Intake and Body, White Adipose Tissue, and Liver Weights. Average energy intakes for the 6 groups over 11 weeks in experiment I are shown in Fig. 1A. Energy intakes in sucrose-supplemented mice were 1.4-fold greater than those in control mice (starch),

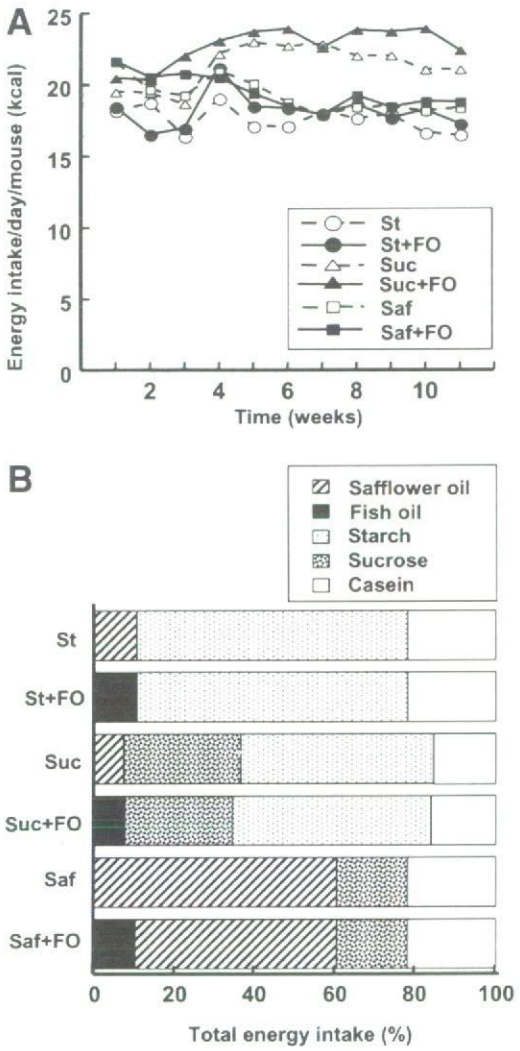

Fig. 1. Daily energy intake and macronutrient intake in experiment I. St, high-starch diet; St+FO, high-starch diet plus fish oil; Suc, high-starch diet plus 20% (wt/wt) sucrose drink; Suc+FO, high-starch diet plus 20% (wt/wt) sucrose drink and fish oil; Saf, high-safflower oil; Saf+FO, high-safflower oil plus fish oil. (A) Daily energy intake. Intakes of food and drinking water were measured daily during the study and were averaged weekly. The data represent the mean daily energy intake. (B) Average energy percentage intakes of macronutrients throughout the study. Safflower oil, fish oil, starch, sucrose, and casein percentages of total energy intake were calculated.

whereas those in HF diet-fed mice were similar to those of control mice. The increased total energy intake in sucrose-supplemented mice was due to the extra energy supply from the sucrose-supplemented drinking water. The macronutrient composition of en% in each group is also shown in Fig. 1B. Fish oil supplementation did not affect the intake of total energy or of other macronutrients.

Increases in body weight were observed in high-safflower oil–fed mice (relative to high-starch–fed mice) (Table 3), although the energy intake was similar in these 2 groups. This discrepancy in body weight increase between groups may be attributable to differences in physical activity level, dietary-induced thermogenesis, or basal metabolic rate. Feeding of 10 en% fish oil did not affect body weight or epididymal, retroperitoneal, mesenteric, or subcutaneous white adipose tissue (WAT) weight in the high-starch diet, sucrose-supplemented, or high-safflower oil-fed mice. However, 2-way ANOVA analysis showed that, among several types of WAT, epididymal WAT was sensitive to fish oil (fish oil effect, $P = 0.010$). Liver weight in sucrose-supplemented and in high-safflower oil-fed mice was 1.20-fold and 1.28-fold, respectively, that in high-starch-fed mice. The effects of fish oil on liver weight differed. Fish oil partially prevented the sucrose-induced increase in liver weight (not significant) but significantly exacerbated the high-safflower oil–induced increase in liver weight.

Fish Oil Prevents Sucrose-Induced Liver TG Accumulation and Exacerbates High-Safflower Oil–Induced Liver TG Accumulation. In parallel with alterations in liver weight, liver TG concentration in sucrose-supplemented mice and in high-safflower oil–fed mice was 1.7-fold and 2.2-fold, respectively, that in high-starch–fed mice (Fig. 2A). The effects of fish oil on liver TG accumulation differed. Fish oil prevented the sucrose-induced increase in liver TG but did not affect the high-safflower oil–induced increase in liver TG. On a whole liver basis, fish oil increased liver TG by 50% in high-safflower oil–fed mice (Fig. 2B). The tuna oil used in this study contained 7% EPA, 24% DHA, and other highly polyunsaturated fatty acids. Other fish oils were also examined. Sardine oil contains 28% EPA and 12% DHA, and a mixture of tuna and sardine oils contains 6% EPA and 13% DHA and is also effective in preventing sucrose-induced hepatic TG accumulation (data not shown).

Oil red O staining confirmed hepatic TG accumulation in both sucrose-supplemented mice and high-safflower oil–fed mice and also confirmed that fish oil prevented sucrose-induced hepatic TG accumulation but not high-safflower oil–induced hepatic TG accumulation (Fig. 3). This beneficial effect of fish oil was also observed in control mice; mild liver TG accumulation was observed in high-starch–fed mice, and this accumulation was prevented by fish oil. Hematoxylin-eosin staining more clearly depicted the microvesicular fatty change within hepatocytes in both sucrose-supplemented mice and high-safflower oil-fed mice (Fig. 4). These changes were not observed in fish oil–supplemented, sucrose-supplemented mice but were observed in fish oil–supplemented, high-safflower oil–fed mice.

Effects of Sucrose Supplementation on Fatty Liver. The mechanisms underlying the development of fatty liver in mice supplemented with sucrose were elucidated by hepatic gene expression profiling. SREBP-1c is a major